MAX-PLANCK-INSTITUT FÜR PLASMAPHYSIK

GARCHING BEI MÜNCHEN

Effect of Parallel Ion Motion in Three-drift-wave Interaction

He Kaifen* and D. Biskamp

IPP 6/233 March 1984

Abstract:

The nonlinear interaction of three drift modes, including parallel ion motion, is discussed analytically and numerically. An intrinsic stochastic interaction between the fluctuating electric field and the parallel ion current is observed and the saturation level is of the expected magnitude.

*Permanent address: Institute of Low Energy Nuclear Physics, Beijing Normal University, Beijing, China

Die nachstehende Arbeit wurde im Rahmen des Vertrages zwischen dem Max-Planck-Institut für Plasmaphysik und der Europäischen Atomgemeinschaft über die Zusammenarbeit auf dem Gebiete der Plasmaphysik durchgeführt.

I. Introduction

Experiments in tokamaks show broad spectra of frequency and wavelength around those of drift waves, indicating a strongly turbulent state. Usually, statistical methods are used to investigate a turbulent state. In recent years, however, progress has been made in understanding the chaotic behaviour of deterministic low-order systems. This suggests a different way to investigate the onset of a turbulent state by using a system of few degrees of freedom. In Ref. [1] Terry and Horton studied the nonlinear interaction of three drift waves from the polarization drift and the convection of density fluctuations. Stationary states have been observed which are either phase-locked steady states or saturated states with stochastic electric field fluctuations. Their results show an apparently intrinsic cause of the onset of turbulence and the applicability of the random phase approximation. The energy fed by electrons into the system passes from the unstable wave to the others through wave-wave coupling. However, if finite parallel (to the magnetic field) wavelengths are permitted, there is another possibility of wave-ion interaction leading to direct transfer of wave energy to kinetic energy of ions. This possibility is proposed in Ref. [2] and further developed in Ref. [3]. It is pointed out that in the linear theory the ions are not resonant when $\omega \gtrsim k_z v_i$ and have little damping effect on the unstable fluctuations, but various nonlinear process may cause the ion motion to be stochastic. In a kinetic description the ions could therefore absorb energy

from the drift wave fed by electrons and damp it. In the present paper we study the effect of parallel ion motion in a low-order system of fluid model to show that the stochasticities of the interaction between the electric field and the parallel ion current, and consequently that of the parallel ion sound wave, may occur intrinsically in a deterministic system. We consider a system of three interacting drift waves including fluctuating parallel ion currents. In Sec. II, model equations are obtained in the limit of weak nonlinearity. A condition is found for the existence of a steady state due to the convective nonlinearity of the parallel current. In Sec. III, we derive a set of rate equations for the amplitudes and phases of both electric fields and parallel ion currents. In these equations, we include the nonlinearities of polarization drift and the convection of density fluctuations as well as that of the convection of parallel current fluctuations. These equations were solved numerically. It is observed that with the change of the rate of phase space volume contraction the stable solution changes from stable steady state to a modulated periodic oscillation and finally to bounded chaotic oscillations. When drift wave parameters are used, the major result is that including the effect of finite parallel current leads to saturation levels in a range as anticipated for drift wave turbulence, and that the results have less dependence on the growth rates chosen, in contrast to the strong parameter-dependent results observed in the case $k_{\parallel} = 0$, treated in [1].

II. Simplified model equations and parametric decay

In the presence of magnetic shear, there is, in general, an ion current J along the magnetic line coupled to the drift wave. The ion density n and the parallel current fluctuation J are determined by the following moment equations [3] [4]:

$$\frac{\partial n'}{\partial t} + \frac{1}{e}\nabla_{\parallel} J + \nabla_{\perp} \cdot \left[n \left(\vec{v}_E + \vec{v}_p \right) \right] = 0, \tag{1}$$

$$\frac{\partial J}{\partial t} + \frac{e}{m}\nabla_{\parallel} p + \frac{ne^2}{m} \nabla_{\parallel}\phi + \vec{v}_E \cdot \nabla_{\perp} J = 0, \tag{2}$$

where

$$\vec{v}_E = - \nabla_{\perp}\phi \times \vec{B}_o / B_o^2,$$

$$\vec{v}_p = - \frac{1}{\omega_{ci} B_o} \left[\left(\vec{v}_E \cdot \nabla_{\perp} \right) \nabla_{\perp}\phi + \frac{\partial \nabla_{\perp}\phi}{\partial t} \right]$$

are the $\vec{E} \times \vec{B}$ and polarization drifts, respectively, $n \equiv n_o + n'$, n_o is the unperturbed ion density, and n' is the density perturbation, $\vec{B}_o$ is the applied magnetic field, P is the ion pressure which will be neglected in the following, e,m are the ion charge and mass, respectively, $\nabla_{\perp}\cdot$ is the divergence in the direction perpendicular to $\vec{e}_z$, and $\nabla_{\parallel}$ is the derivative along the magnetic field; ϕ is the fluctuating electric potential and $\omega_{ci} \equiv \frac{eB_o}{mc}$ is the ion

cyclotron frequency.

We use the following units: $\frac{T}{n_o e}\frac{\rho_s}{L_n}$ for ϕ, $n_o e c_s \frac{\rho_s}{L_n}$ for J, L_n/c_s for t, and $1/L_n$ and $1/\rho_s$ for $\nabla_{\parallel}$ and $\nabla_{\perp}$, respectively. Here L_n is the characteristic length of the density gradient and $\rho_s \equiv c_s/\omega_{ci}$, where c_s is the sound speed.

If the response of electrons is assumed to be linear, then by using the quasi-neutrality condition the Fourier component of the density fluctuation $n'_{k,\omega}$ is related to that of the fluctuating potential $\phi_{k,\omega}$ by the following expression:

$$n'_{k,\omega} = \phi_{k,\omega} \quad (1 - i\delta_{k,\omega})$$

Here, $\delta_{k,\omega}$ results from the nonadiabatic response of the electrons.

Since the mechanisms for the nonlinear interaction coming from the terms $\nabla \cdot n (\vec{v}_E + \vec{v}_p)$ have already been studied elsewhere (e.g. Ref. [6]), we should like to shed some light on the effect of the third nonlinear term, $\vec{v}_E \cdot \nabla J$. In this section the nonlinear terms in eq. (1) are omitted but are included in the numerical calculation in the next section. In this case, eq. (1) and eq. (2) reduce to (writing $i\delta_k \frac{\partial \phi_k}{\partial t} = \gamma_k \phi_k$)

$$\frac{\partial \phi_{\vec{k}}}{\partial t} = \gamma_{\vec{k}} \phi_{\vec{k}} - i\, k_y\, \phi_{\vec{k}} - i\, k_{\parallel} J_{\vec{k}} \quad , \qquad (3)$$

$$\frac{\partial J_{\vec{k}}}{\partial t} = - i\, k_{\parallel} \phi_{\vec{k}} + \sum_{\vec{k}'+\vec{k}''=\vec{k}} (\vec{k}'_{\perp} \times \vec{k}''_{\perp}) \cdot \hat{n}\, \phi_{\vec{k}'}\, J_{\vec{k}''} \,. \qquad (4)$$

In a dissipationless case, $\gamma_j = 0$, it is easy to see that the total energy W is conserved:

$$\frac{dW}{dt} \equiv \frac{d}{dt} \sum_{\vec{k}} \left(|\phi_{\vec{k}}|^2 + |J_{\vec{k}}|^2 \right) = 0. \qquad (5)$$

The linear dispersion relation derived from eq.(3) and eq. (4) is

$$\omega^2 - (k_y + i\,\gamma)\,\omega - K_{\parallel}^2 = 0 \,, \qquad (6)$$

where $K_{\parallel}$ is the parallel component of $\vec{k}$ along the magnetic line. (in the following the subscript of $K_{\parallel}$ is omitted). When $K \ll k_y$ and $\gamma \ll \omega$, one can find a solution of the dispersion relation (6) around the drift frequency:

$$\omega_{\vec{k}} = k_y \left(1 + \frac{K^2}{k_y^2}\right). \qquad (7)$$

We now investigate the simplest nonlinear interaction, i.e. three-wave interaction. The three modes form a triangle with $\vec{k}_1 + \vec{k}_2 + \vec{k}_3 = 0$. Their projected components on the magnetic line $\vec{B}$ are K_1, K_2, K_3 , respectively. We express the j-th mode of ϕ in terms of real amplitude a_j and real phase angle α_j:

$$\phi_j(t) = a_j(t) \exp\{-i\alpha_j(t)\} . \qquad (8)$$

$\alpha_j(t)$ can be divided into two parts, $\alpha_j(t) = \omega_j t - \tilde{\alpha}_j(t)$, on the assumption that $\dot{\tilde{\alpha}}_j(t) << \omega_j$, where ω_j is a constant (eq. (7).).

If weak nonlinearity is assumed, eq. (4) for the j-th mode can be written as

$$\frac{dJ_j}{dt} = - iK_j\phi_j - A\left(\frac{K_1}{\omega_1} - \frac{K_m}{\omega_m}\right)\phi_1^* \phi_m^* \qquad (9)$$

ϕ_j^* is the complex conjugate of ϕ_j. Here we have neglected higher orders in the nonlinear terms.

Substituting eq. (8) in the time derivative of eq. (3), using relations (9) and (7) and neglecting small terms, we obtain the model equations for the amplitude a_j and phase α_j:

$$\frac{da_j}{dt} = \frac{\gamma_j}{1+\frac{K_j^2}{\omega_j^2}} a_j - \frac{A}{1+\frac{K_j^2}{\omega_j^2}} \frac{K_j}{\omega_j}\left(\frac{K_1}{\omega_1} - \frac{K_m}{\omega_m}\right) a_1 a_m \cos\alpha, \qquad (10)$$

$$\frac{d\alpha_j}{dt} = \omega_j + \frac{A}{1+\frac{K_j^2}{\omega_j^2}} \frac{K_j}{\omega_j}\left(\frac{K_1}{\omega_1} - \frac{K_m}{\omega_m}\right) \frac{a_1 a_m}{a_j} \sin\alpha . \qquad (11)$$

The summation of eq. (11) for j = 1,2,3 gives

$$\frac{d\alpha}{dt} = \Sigma\omega_j + A \sum_{j,1,m} \frac{1}{1+K_j^2/\omega_j^2} \frac{K_j}{\omega_j} \left(\frac{K_1}{\omega_1} - \frac{K_m}{\omega_m}\right) \frac{a_1 a_m}{a_j} \sin\alpha \quad (12)$$

Here, $\alpha \equiv \alpha_1 + \alpha_2 + \alpha_3$, $A = \frac{1}{2} \vec{k}_1 \times \vec{k}_2 \cdot \hat{n}$, $\{j,1,m\}$ is a cyclic permutation of $\{1,2,3\}$.

Let us denote $\hat{D}_j \equiv \frac{D_j}{1+K_j^2/\omega_j^2}$, where

$$D_j \equiv \frac{K_j}{\omega_j} \left(\frac{K_1}{\omega_1} - \frac{K_m}{\omega_m}\right) \quad (13)$$

with $\sum_{j=1}^{3} D_j = 0$, and $\hat{\gamma}_j \equiv \frac{\gamma_j}{1+K_j^2/\omega_j^2}$. Equations (10) and (12) have the same form as that discussed in [1] with real susceptibilities. In a dissipationless case it is therefore easy to find from eqs. (10) and (12) the conservation laws that are similar in form to those in [1] for real susceptibility, and a solution in terms of elliptical functions can also be obtained. The details are omitted here.

In a similar way, one can also find simultaneous conditions for the existence of a steady state for eqs. (10) and (12) in a driven-damped system:

$$\text{sgn}(\gamma_j) = -\text{sgn}(\gamma_1) = -\text{sgn}(\gamma_m) , \quad (14A)$$

$$\text{sgn}(D_j) = -\text{sgn}(D_1) = -\text{sgn}(D_m) , \quad (14B)$$

where sgn (x) is the sign of x. Here we have obtained formally the same condition as in [1]. But, in the present case, the quantity for

the criterion is D_j, which is a function of phase velocities along magnetic lines instead of a function of wavelengths.

If it is assumed that the j-th wave has the intermediate phase velocity, that is,

$$\frac{Km}{\omega_m} < \frac{Kj}{\omega_j} < \frac{Kl}{\omega_l}$$

(or the inverse inequality), then D_j always has a sign different to that of D_l and D_m. Consequently, condition (14) tells us that only in two circumstances can a steady state exist: the wave with intermediate phase velocity grows and the faster and slower waves are damped, or the wave of intermediate phase velocity is damped, while the other two waves grow.

It follows from this discussion that a large wave can parametrically decay into two waves, the one with higher parallel phase velocity, the other with lower phase velocity. In a cascade process the decay of a large-amplitude wave would thus lead to a broad spectrum in wavelength and frequency.

III. Numerical solutions of the complete equations

In deriving the model equations (10) and (11) in the last section, we used eq. (9) with the current J in the nonlinear term $\vec{v}_E \cdot \nabla J$ being replaced by its linear value $\frac{K}{\omega_k} \phi$, where ω_k is the linear frequency. However, if the amplitudes are large, this substitution is in general not valid. One must allow for a nonlinear change of the frequencies and growth rates, which strongly affects the possibility of parametric decay, discussed in Sec. II. Moreover, the fluctuating field and the parallel current may usually have different phases. We therefore assume ϕ_j and J_j in the more general forms

$$\phi_j(t) = a_j(t) \exp \{- i\alpha_j(t)\} , \tag{15}$$

$$J_j(t) = b_j(t) \exp \{- i\beta_j(t)\} \tag{16}$$

Taking into account the polarization drift and the density convection nonlinearities as well as the nonlinearity resulting from the convection of the parallel current, we obtain from eqs. (1) and (2) a set of rate equations for the amplitudes and phases of both ϕ_j and J_j:

$$\frac{da_j}{dt} = \gamma_j a_j - K_j b_j \sin \theta_j - A(F_j \cos\alpha - G_j \sin\alpha)\, a_l a_m , \tag{17}$$

$$\frac{db_j}{dt} = K_j a_j \sin\theta_j + 2A\left[a_1 b_m \cos(\beta-\theta_1) - a_m b_1 \cos(\beta-\theta_m)\right], \quad (18)$$

$$\frac{d\theta_j}{dt} = -\omega_j - \frac{K_j b_j}{a_j}\cos\theta_j + \frac{K_j a_j}{b_j}\cos\theta_j -$$

$$- A\left[F_j \sin\alpha + G_j \cos\alpha\right]\frac{a_1 a_m}{a_j} -$$

$$- 2A\left[\frac{a_1 b_m}{b_j}\sin(\beta-\theta_1) - \frac{a_m b_1}{b_j}\sin(\beta-\theta_m)\right], \quad (19)$$

$$\frac{d\beta}{dt} = \sum_{j=1}^{3}\frac{K_j a_j}{b_j}\cos\theta_j - 2A\sum_{j,1,m}\left[\frac{a_1 b_m}{b_j}\sin(\beta-\theta_1) -\right.$$

$$\left. - \frac{a_m b_1}{b_j}\sin(\beta-\theta_m)\right], \quad (20)$$

for the three-wave interaction. The three waves have the same triangular relation as in Sec. II., $\theta_j = \beta_j - \alpha_j$ is the phase difference between J_j and ϕ_j, $\beta \equiv \beta_1 + \beta_2 + \beta_3$, $\alpha \equiv \alpha_1 + \alpha_2 + \alpha_3 = \beta - \theta_1 - \theta_2 - \theta_3$, and F_j and G_j are the contributions of the $\vec{v}_E \cdot \nabla\vec{v}_E$ part of the polarization drift and of the $\vec{v}_E \cdot \nabla n'$ convection of the density fluctuations, respectively, $F_j = (k_\perp)_1^2 - (k_\perp)_m^2$, and G_j is chosen in accordance with linear drift wave theory, $G_j = \delta_o\left[(k_y\, k_\perp^2)_1 - (k_y\, k_\perp^2)_m\right]$ as in [1]. The functions F_j and G_j have the properties that $\sum_{j=1}^{3} F_j = 0$ and $\sum_{j=1}^{3} G_j = 0$. Again, {j,1,m} is a cyclic permutation of {1,2,3}.

The energy balance can be derived from eqs. (17) and (18). The rate of change of the total energy of the system is

$$\frac{dW}{dt} \equiv \frac{d}{dt} \frac{1}{2} \sum_{j=1}^{3} (a_j^2 + b_j^2)$$

$$= \sum_{j=1}^{3} \gamma_j a_j^2 \quad . \tag{21}$$

In the present case we have a phase space of 10 dimensions with the volume element $dV = da_1^2 da_2^2 da_3^2 db_1^2 db_2^2 db_3^2 d\theta_1 d\theta_2 d\theta_3 d\beta$. The rate of change of V calculated from eqs. (17) - (20) is

$$\frac{dV}{dt} = \sum_{j=1}^{3} \{\frac{1}{a_j} \frac{\partial}{\partial a_j} (a_j \frac{da_j}{dt}) + \frac{1}{b_j} \frac{\partial}{\partial b_j} (b_j \frac{db_j}{dt}) + \frac{\partial}{\partial \theta_j} (\frac{d\theta_j}{dt})\}$$

$$+ \frac{1}{\beta} \frac{d\beta}{dt} = \sum_{j=1}^{3} 2\gamma_j . \tag{22}$$

When $\gamma_t \equiv \gamma_1 + \gamma_2 + \gamma_3 < o$, the volume in phase space contracts, which is a necessary condition for the existence of a stationary state.

Numerical calculations were made for the coupled equations (17) - (20). First we allow the parameters F_j, G_j, ω_j, γ_j to be arbitrarily chosen and investigate the general properties of the solution of the equations, particularly the existence of steady

states. The conditions for the existence of steady state deduced from Ref. [1] and from the last section for different nonlinear terms are briefly recalled:

$$\text{sgn}\ (\gamma_j) = -\ \text{sgn}\ (\gamma_1) = -\ \text{sgn}\ (\gamma_m)\ , \tag{23A}$$

$$\text{sgn}\ (H_j) = -\ \text{sgn}\ (H_1) = -\ \text{sgn}\ (H_m)\ , \tag{23B}$$

where, $H_j = F_j$ if $G_j = D_j = 0$, $H_j = G_j$ if $F_j = D_j = 0$, $H_j = D_j$ if $F_j = G_j = 0$. For the case of no parallel ion current, it was concluded in [1] that a steady state would be reached if both F_j's and G_j's satisfy the condition (23). We now fix F_j's and G_j's to satisfy the condition (23), i.e., if we switch off the parallel current, the system could have a steady state. We then study the effect of parallel current in the following cases: 1) The wave which has the intermediate parallel phase velocity is the driven mode. (2) The faster wave is the driven mode. (3) The slower wave is the driven mode. Apparently in case (1) the condition (23) is satisfied for D_j's as well as for F_j's and G_j's. But in cases (2) and (3) the condition (23) is only satisfied for F_j's and G_j's, but not for D_j's. A phase-locked steady state is found numerically in case (1) with $\gamma_t = -\ 0.1791$. The result is given in Fig. 1. In the final steady state all the amplitudes of either the fluctuating field or the current approach constants, and so do the phase differences θ_j's and phase α.

But in cases (2) and (3), only turbulent states are observed. Figure 2 shows a result of case (3) as an example.

To study the stability of a steady state, we take the solutions which are obtained by solving the stationary equations ($\dot{a}_j = \dot{b}_j = \dot{\theta}_j = \dot{\beta} = 0$, $j = 1,2,3$, in eqs. (17) - (21)) as initial conditions and calculate its time evolution. Figures 3 - 7 give a series of results when γ_t ($\equiv \gamma_1 + \gamma_2 + \gamma_3$) is increased from $-.01491$ to -0.0991. With $\gamma_t = -0.1791$, the steady state is stable, as can be seen in Fig. 1. When γ_t is larger than γ_c ($\cong -0.1496$), the stationary solution loses its stability and periodic oscillation is observed (Fig. 3, $\gamma_t = -0.1491$). Then with a larger γ_t (Fig. 4 , $\gamma_t = -0.1441$) a slow periodic modulation of the fast oscillation appears. It is very likely that the trajectory is attracted to a two-dimensional torus in phase space.[5] Meanwhile, in Fig. 4(e) one can see evidence of the appearance of the second frequency. When γ_t is further increased, both the modulation frequency and the modulation amplitude increase, but the basic fast oscillation frequency of the amplitudes is almost unchanged (Fig. 5, $\gamma_t = -0.1391$). When $\gamma_t = -0.1291$, it is observed that the chaotic and regular behaviours occur alternatively (Fig. 6). This is characteristic of intermittency.[7] Finally, at higher γ_t, it is observed that the trajectory behaves chaotically ($\gamma_t = -0.0991$, Fig. 7). In contrast to the exponentially increasing envelope observed in [1], the amplitudes are bounded in our case.

When K_j's are twice as large as that in Fig. 1, at higher growth rate $\gamma_t = -0.1391$ we still have a stable steady state.

And only when γ_t is as high as about - 0.1091 can a turbulent solution be obtained. On the other hand, when K_j's are halved, a turbulent state starts at smaller $\gamma_t (< - 0.1791)$, and the existence of a stable steady state needs stronger damping. When K_j's $\to 0$, one could expect the unbounded unstable steady state observed in Ref. [1].

We also made numerical calculations with F_j, G_j, ω_j chosen according to the linear theory of drift waves but with γ_j's still being free parameters. Saturated states with stochastic phases and amplitudes of both the fluctuating fields and the parallel currents were observed. Figures 8 (a), (b) give the time evolutions of the amplitudes of ϕ_j and J_j of the three modes, respectively, (c) gives the phase difference θ_j of one mode, and (d) gives the phase α. γ_t in the plots is - 0.01584. It is clear from the plots that in the linear stage the linearly unstable mode grows exponentially, while the other damped modes decrease. When the growing amplitude is large enough, the nonlinear interaction becomes dominant and a turbulent stationary state is set up with all a_j's and also b_j's of the same order on the average. At this stage, the phase difference θ_j between ϕ_j and J_j becomes very irregular, and so does β(or α).

Different behaviours occur as growth rates γ_j's change. We vary the driving rate γ_1 and keep the two damping rates γ_2 and γ_3 fixed, so that the total $\gamma_t \equiv \gamma_1 + \gamma_2 + \gamma_3$ is changed, too. In a case of

strong damping rate γ_t(- 0.05064), the picture is a little different from Fig. 8. From time to time the interacting amplitudes are almost damped when they are excited again. At the time when the modes are excited, the phase difference θ_j undergoes sudden oscillations. In this way, the system is kept at a certain turbulent level.

Figure 9 shows the average amplitude $\bar{a} \equiv (\sum_{j=1}^{3} \int_{\Delta t} a_j^2(t)dt/\Delta t)^{1/2}$ versus $|\gamma_t|$. The solid circles are of the model of eqs. (17) - (20). In this group of runs we use K_j's ~ 0.5. For all $\gamma_t < 0$, we obtain saturated states. Since Δt used for the average is finite and the behaviour in this case is very irregular with strong bursts, in particular when $\gamma_t \to 0$ and $\vec{K}$'s $\to 0$, the obtained $\bar{a}$ values in Fig. 9 and in the following Fig. 11 and Table 1 are more qualitative than quantitative. Roughly speaking, in Fig. 9 $\bar{a}$ increases almost linearly with γ_t. And the average amplitude $\bar{a}$'s are in the range $\lesssim 10$. This value is much lower than that predicted by the model without current and is of the magnitude usually estimated for drift-wave turbulence.

For comparison with our model of nonlinear current (n.l.c), we also calculated the models where the parallel current is completely neglected (n.c.), and where the current is linear (l.c.), i.e. neglecting the nonlinear term $\vec{v}_E \cdot \nabla J$ in the J equation but including the other two nonlinear terms in the ϕ equation. Table 1 gives the comparison of the three models for several γ_t's.

In the cases without current, which is what Ref. [1] has con-

sidered, we find that the range in γ where one can observe stochastic saturation is narrower than with current, and that the level of saturation, if it exists, is much higher than in our model. If in the n.c. model a moderate γ_t is used (e.g. $\gamma_t = -0.02198$ or -0.01578, see Fig. 10), it seems that one can find stochastic saturation, but the average amplitude is about one order of magnitude higher than in our model (Fig. 8). When γ_t is increased above about -0.01 (e.g. $\gamma_t = -0.00969$), the amplitudes continue to grow on the average and no turbulent saturation is found. However, for the n.l.c. model with the same parameters and finite K_j's we still get a rather low saturation level with $\bar{a}$ around 5. When damping is strong (e.g. $\gamma_t = -0.05064$), the results from the n.c. model show apparently coherent amplitude oscillation. It can be seen from Table 1 that, apart from their relatively low values, the saturation levels of the n.l.c. model are less sensitive to changes of the parameter γ_t. On the other hand, for the n.c. model, when γ_t is slightly changed, the result changes dramatically.

The computation shows that the nonlinear term $\vec{v}_E \cdot \nabla J$ by itself cannot lead to saturation in the present model if the nonlinear terms are neglected in the ϕ equation. In this case, the individual modes keep growing or decaying, depending on their phases. Nevertheless, the nonlinearity $\vec{v}_E \cdot \nabla J$ still plays an obvious role in the process of saturation in the complete model. In Fig. 9 it can be seen that for the same parameters the average amplitude $\bar{a}$ of the l.c. model (without $\vec{v}_E \cdot \nabla J$) is several times as large as that of the n.l.c. model (including $\vec{v}_E \cdot \nabla J$). One can imagine the way in which the nonlinear term $\vec{v}_E \cdot \nabla J$

plays a role in reaching saturation. It is the fact that the two nonlinear terms in the ϕ equation excite a variety of different frequencies and amplitudes which provides the condition for the parametric decay in the third nonlinear term $\vec{v}_E \cdot \nabla J$. In turn, this decay excites even more values of frequency and amplitude, which keeps the system at a lower saturation level.

Figure 11 gives the average amplitude $\bar{a}$ versus K/k_y. The suppression of $\bar{a}$ due to the presence of finite parallel wave number K is obvious. With decreasing K, the average amplitude $\bar{a}$ rapidly increases. In the case of small K_j's, after the first parametric decay the parallel current is still small, and the amplitudes appear coherent, which is characteristic of the same stage in the case without current. After the current has become large enough to compete with the unstable electric field, saturation can be reached. If K approaches zero, the behaviour returns to the n.c. case.

Figures 12(a)(b) present the frequency spectra of the fluctuating electric field ϕ_j and the parallel current J_j of one mode (mode 2), respectively. The parameters are the same as in Fig. 8. For typical turbulence levels the spectra are broad with widths $\Delta\omega$ exceeding the drift frequency ω_j, $\Delta\omega > \omega_j$. The broad spectrum of J_j shows the random motion of ion fluid caused by the nonlinear interaction.

Figure 13 gives the entropy-like quantity [6]

$$H = \frac{1}{n\tau} \sum_{i=1}^{n} \ln \frac{|di|}{|d|} ,$$

corresponding to the case of Fig. 8, where $|d|$ is the initial separation of two neighbouring trajetories in phase space, $|d_i|$ is their separation at the end of the i-th period of duration τ. This entropy-like quantity is related to the Kolmogorov entropy. A positive value of H arises from the exponential separation of two initially neighbouring trajectories in phase space and gives a measure of the stochasticity of the system.

IV. Conclusions

We have investigated the three-drift-wave interaction, taking into account the effect of fluctuating parallel ion current. In the equations we have included the convective nonlinearity of parallel current in addition to the $\vec{E} \times \vec{B}$ and polarization drift nonlinearities.

In the case of weak nonlinearity we find analytically a decay mechanism considering only the nonlinear term in the J equation. The condition for the decay is related to the parallel phase velocities of the three waves.

For a contracting flow in phase space ($\gamma_t < o$) we have numerically observed several different types of solutions: phase-locked steady states bifurcated to modulated oscillations, as well as bounded chaotic

oscillation, depending on the phase space contraction rate γ_t.

Numerical calculations of the time evolution in the present model show the nonlinear stabilizing effect of parallel wavelength which is the result of the stochastic interaction between fluctuating fields and ion sound waves. When applied to actual drift wave parameters, the saturated level obtained is relatively insensitive to the variation of γ_t. And with reasonable values of parallel wave numbers, the saturation occurs at the anticipated level.

Acknowledgement

One of the authors (K.H.) is grateful to A. Salat for the heuristic discussion and to O. De Barbieri, R. Meyer-Spasche and H. Welter for their help with the numerical calculation.

References

[1] P. Terry and W. Horton, Phys. Fluids 25, 491 (1982)

[2] T.H. Dupree, Phys. Fluids 10, 1049 (1966)

[3] T.H. Dupree and D.J. Tetreault, Phys. Fluids 21 , 425 (1978)

[4] A. Hasegawa and K. Mima, Phys. Fluids 21, 87 (1978)

[5] E. Ott, Rev. of Mod. Phys. 53, 655 (1981)

[6] G. Benettin, L. Galgani and J.M. Strelcyn, Phys. Rev. A 14, 2338 (1976)

[7] B. Hu and J. Rudnick, Phys. Rev. Lett. 48, 1645 (1982)

Fig. 1 Steady state, the wave with the intermediate velocity as the driven mode.(a) a_j's, (b) b_j's (j=1,2,3), (c) $\cos\theta_1$, (d) $\cos\alpha$. $\vec{k}_1$ = (0.8935, 1.2048), $\vec{k}_2$ = (-0.4436, -0.8032), $\vec{k}_3$ = (-0.4499, -0.4016), F = (0.297, -0.237, - 0.06), G = (-0.2247, 0.2012, 0.0235), K = (0.78253, - 0.52169, - 0.26084), ω = (0.47065, -0.25615, - 0.2945), γ = (0.09,- 0.25, - 0.0191).

Fig. 2 Turbulent state, fastest wave as the driven mode.(a) a_j's, (b) b_j's (j = 1,2,3), (c) $\cos\theta_1$, (d) $\cos\alpha$. K = (-0.26084, - 0.52169, 0.78253), ω = (-0.2945, -0.25615, 0.47065), other parameters as in Fig. 1.

Fig. 3 Marginally unstable steady state, γ_t = -0.1491. (a) a_j's, (b) b_j's (j = 1,2,3), (c) $\cos\theta_j$, (d) $\cos\alpha$.

Fig. 4 Solution of modulated oscillation type, γ_t = -0.1441. (a) a_1, (b) b_1, (c) $\cos\theta_1$, (d) $\cos\alpha$, (e) detail of $\cos\theta_1$.

Fig. 5 Solution of modulated oscillation type , γ_t = -0.1391. (a) a_1, (b) $\cos\theta_1$.

Fig. 6 Solution of alternatively chaotic and regular behaviours γ_t = -0.1291. (a) a_1,(b) $\cos\theta_1$.

Fig. 7 Bounded chaotic solution, γ_t = - 0.0991. (a) a_1, (b) $\cos\theta_1$.

Fig. 8 Time evolution for the complete model (n.1.c) with drift wave parameters. (a) a_j's, (b) b_j's (j=1,2,3) , (c) $\cos\theta_1$, (d) $\cos\alpha$, $\vec{k}_1$ = (0.8935, 1.2048), $\vec{k}_2$ = (-0.4436, -0.8032), $\vec{k}_3$ = (-0.4499, -0.4016), K = (0.78253, -0.52169, -0.26084), γ_t = -0.01584.

Fig. 9 Average amplitude $\bar{a}$ versus $|\gamma_t|$ for different models: solid circle - the complete model of eqs.(17) - (20) (n.l.c.), open circle - the model with linear current (1.c.), cross - the model without current (n.c.)

Fig. 10 Time evolution of the amplitudes for the model without current (n.c.), drift wave parameters. $\vec{k}_1 = (0.8935, 1.2048)$, $\vec{k}_2 = (-0.4436, -0.8032)$, $\vec{k}_3 = (-0.4499, -0.4016)$, $\gamma_t = -0.01584$.

Fig. 11 Average amplitude $\bar{a}$ versus K/k_y. $\gamma_t = -0.01584$.

Fig. 12 Fourier spectra from fast Fourier transform of (a) $\phi_2(t)=a_2(t)e^{-i\alpha_2(t)}$ and (b) $J_2(t) = b_2(t)\, e^{-i\beta_2(t)}$ for the same case as in Fig. 8.

Fig. 13 Entropy-like quantity for the same case as in Fig. 8.

Table 1 The comparison between models of (a) nonlinear current (n.l.e), (b) linear current (l.c) and (c) no current (n.c) for different γ_t

γ_t	model	$\bar{a}$	state
-0.05064	n.l.c.	<0.886	saturation
	l.c.	4.74	saturation
	n.c.	3.70	saturation (coherent amplitudes)
-0.03426	n.l.c.	<0.935	saturation
	l.c.	10.79	saturation
	n.c.	6.15	saturation (coherent amplitudes)
-0.02198	n.l.c.	2.92	saturation
	l.c.	13.95	saturation
	n.c.	17.88	saturation
-0.01584	n.l.c.	3.54	saturation
	l.c.	12.75	saturation
	n.c.	60.97	saturation
-0.00969	n.l.c.	4.67	saturation
	l.c.	14.25	saturation
	n.c.	-	no saturation observed
-0.00485	n.l.c.	9.97	saturation
	l.c.	30.14	saturation
	n.c.	-	no saturation observed

The other parameters are:

$\vec{k}_1 = (0.8935, \ 1.2048)$
$\vec{k}_2 = (-0.4436, -0.8032)$
$\vec{k}_3 = (-0.4499, -0.4016)$
$K_1 = 0.78253$
$K_2 = -0.52169$
$K_3 = -0.26084$

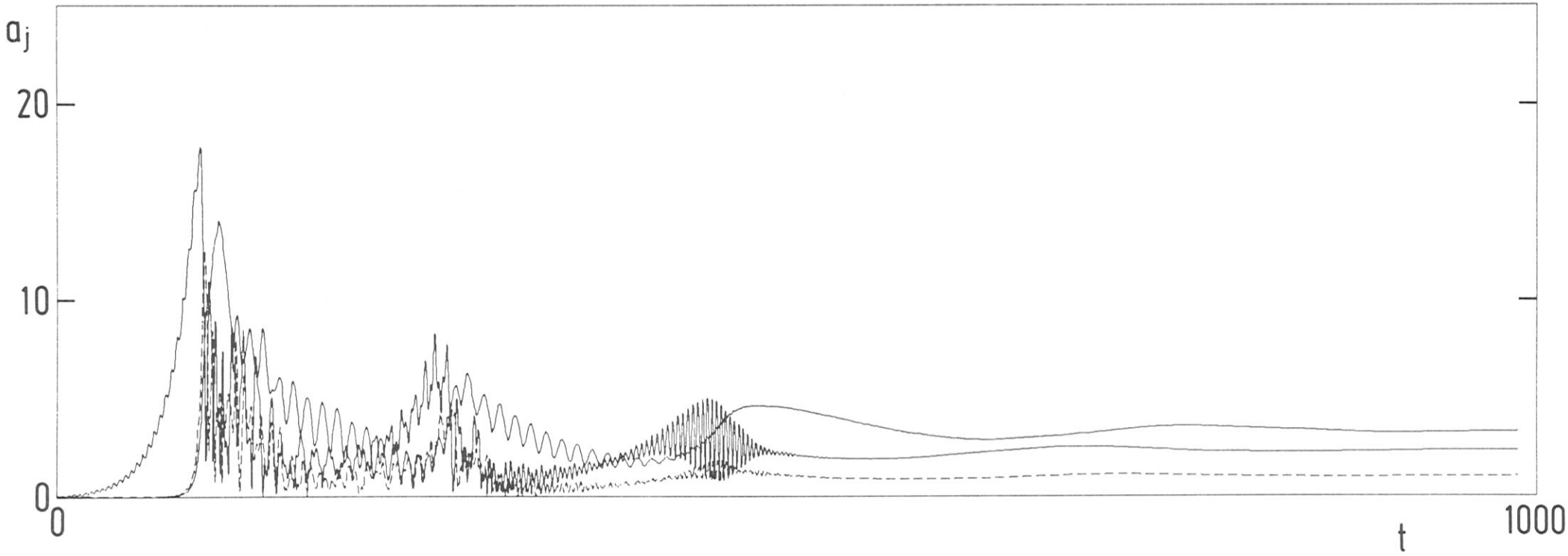

Fig. 1(a)

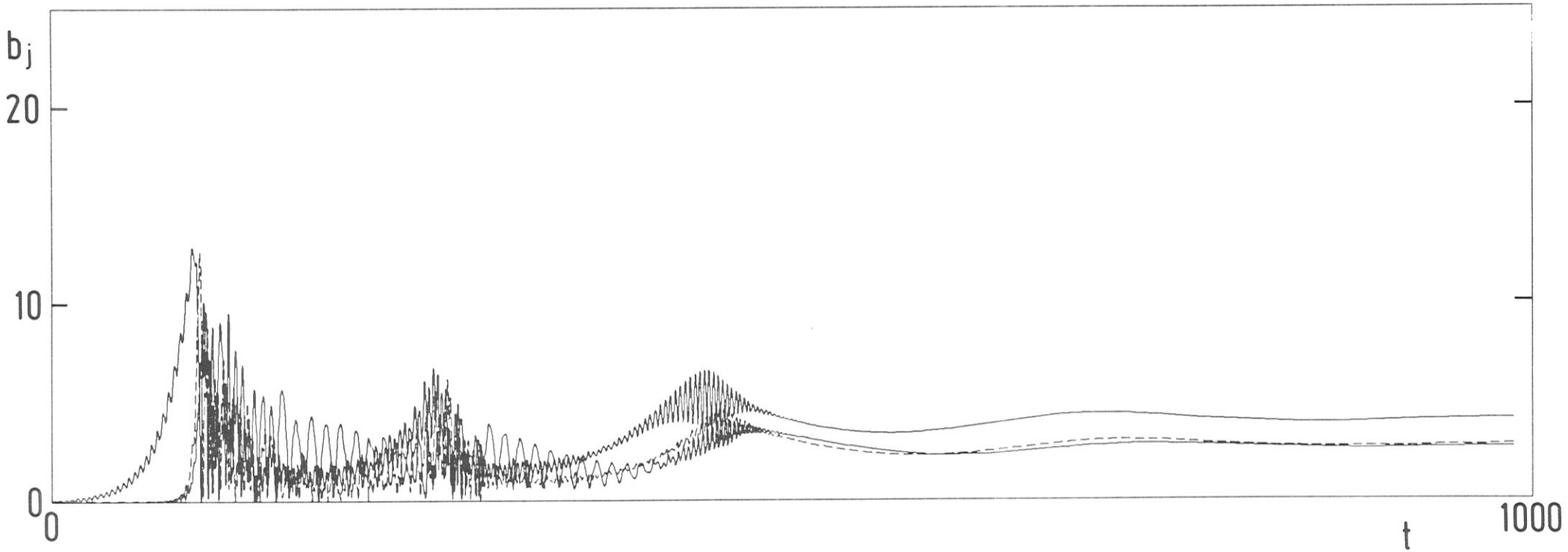

Fig. 1(b)

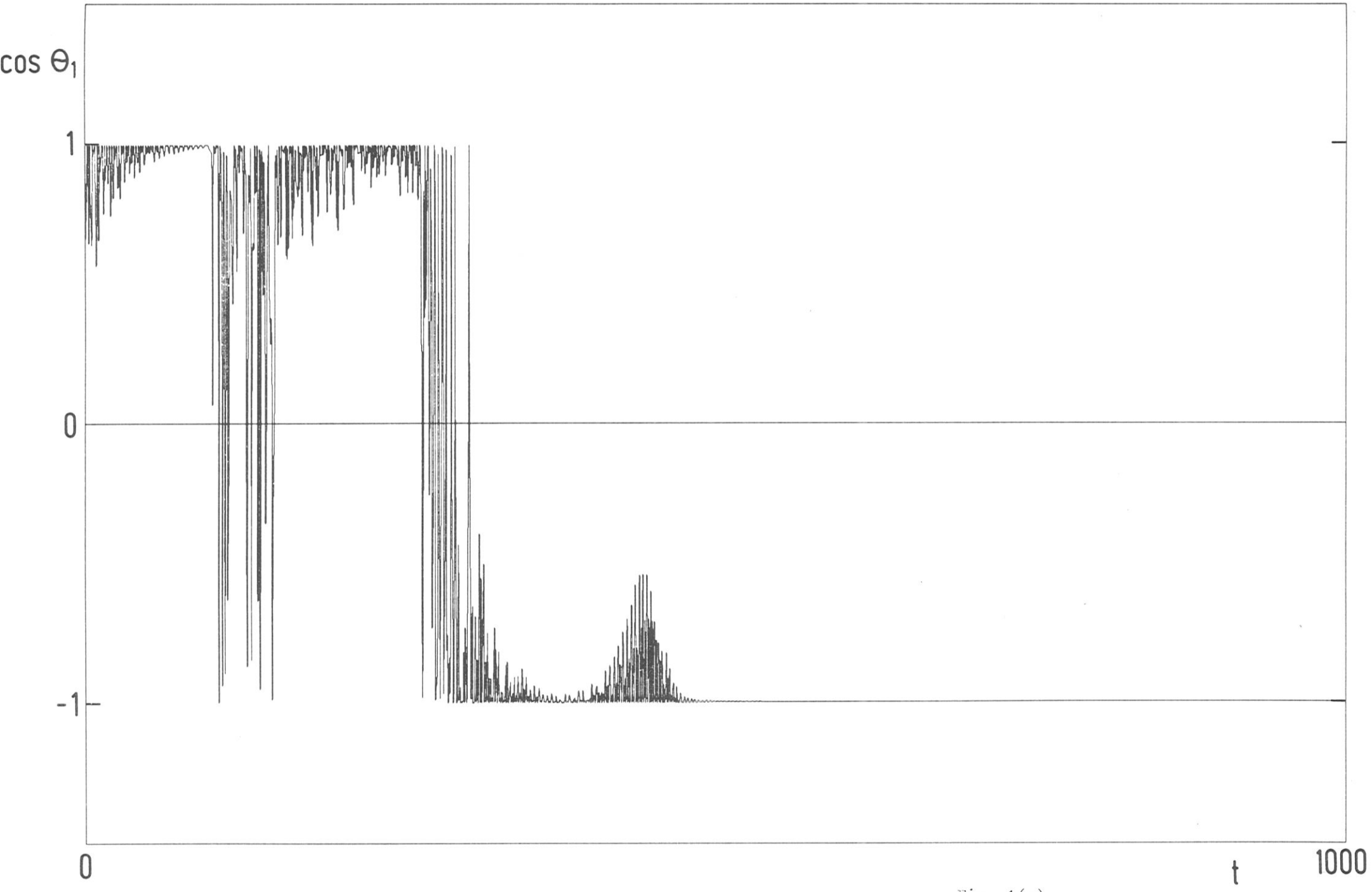

Fig. 1(c)

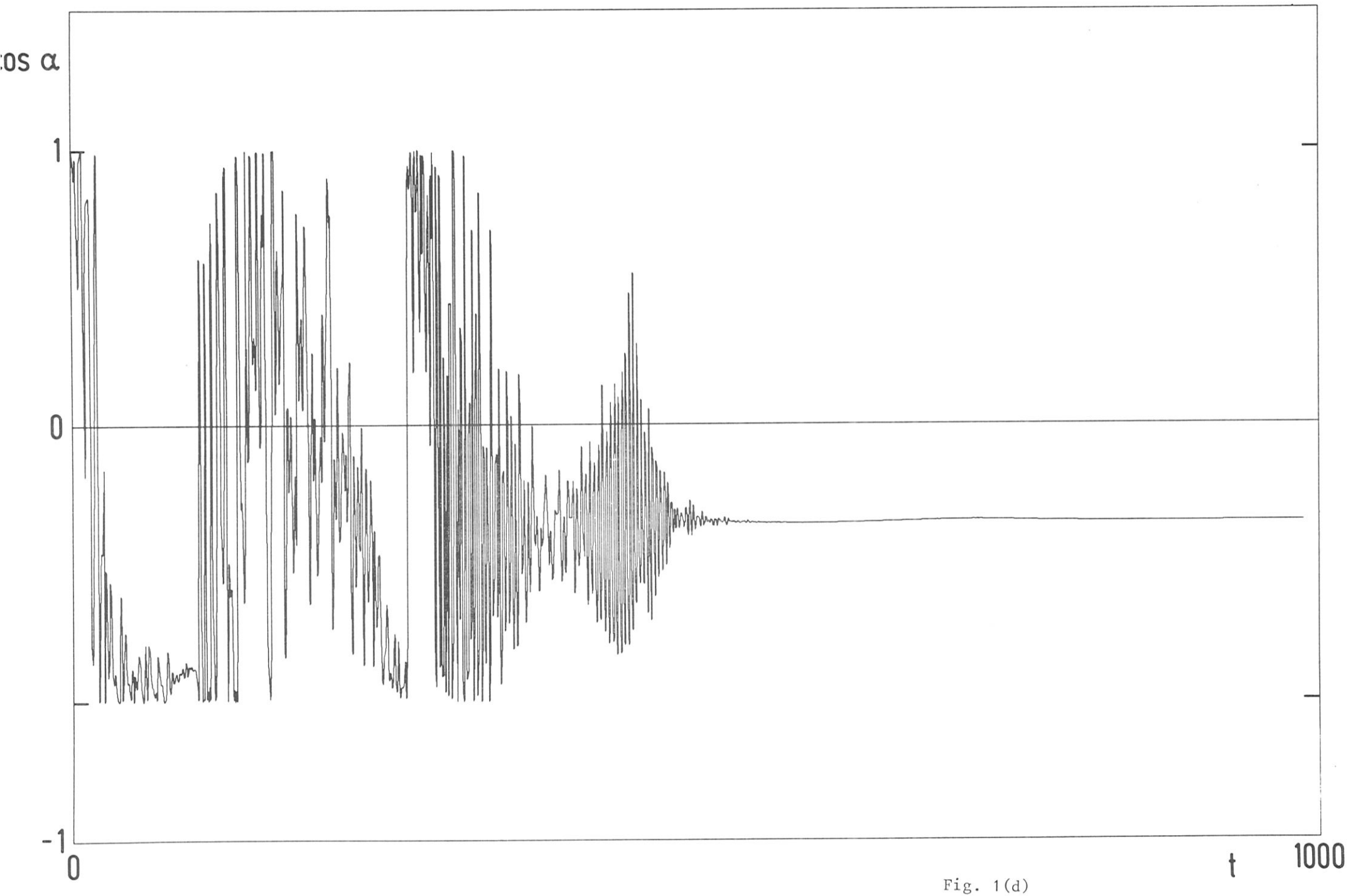

Fig. 1(d)

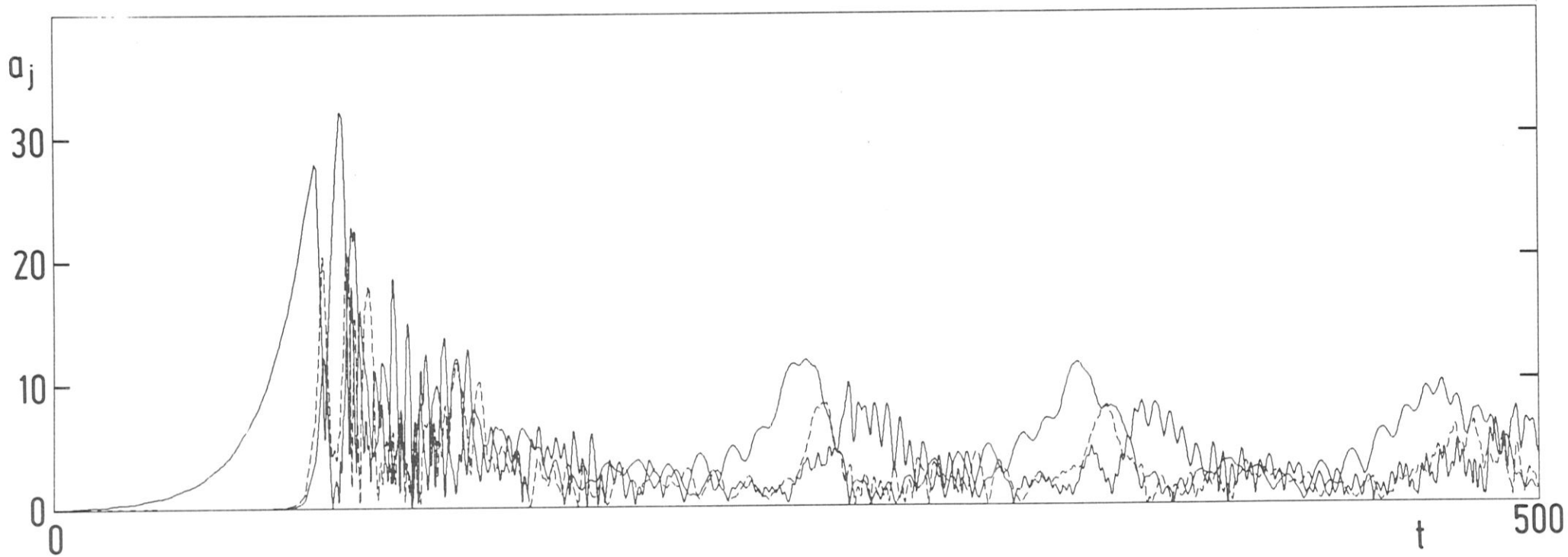

Fig. 2(a)

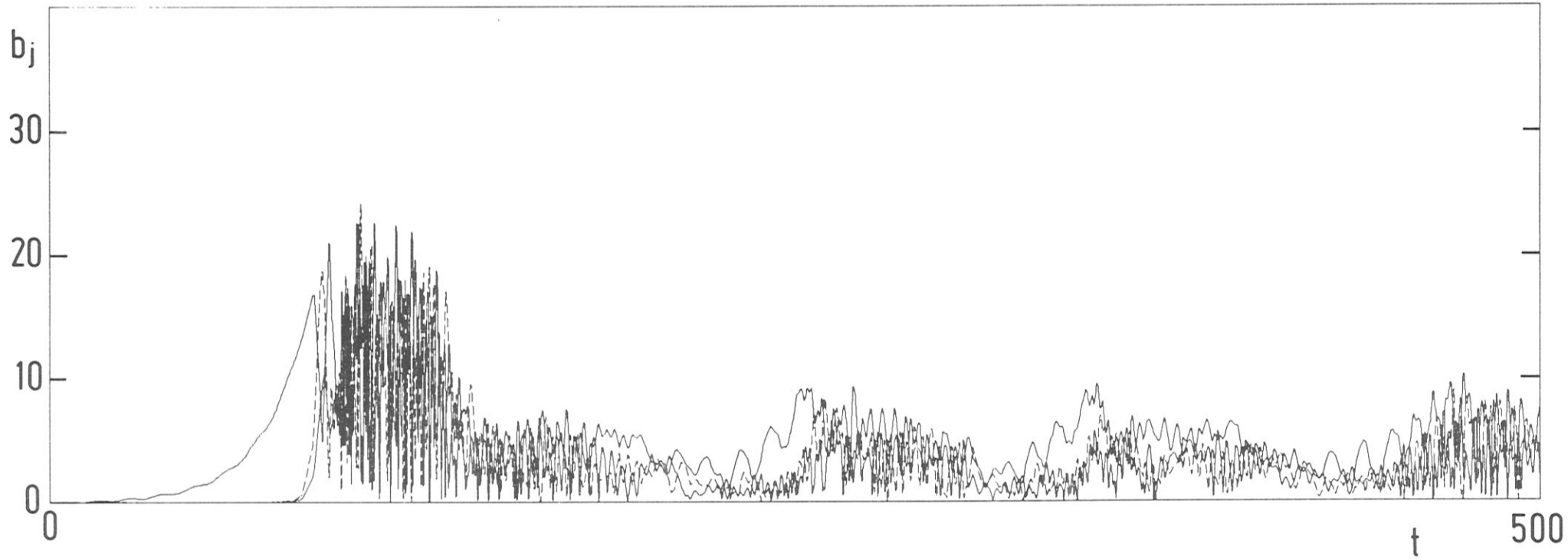

Fig. 2(b)

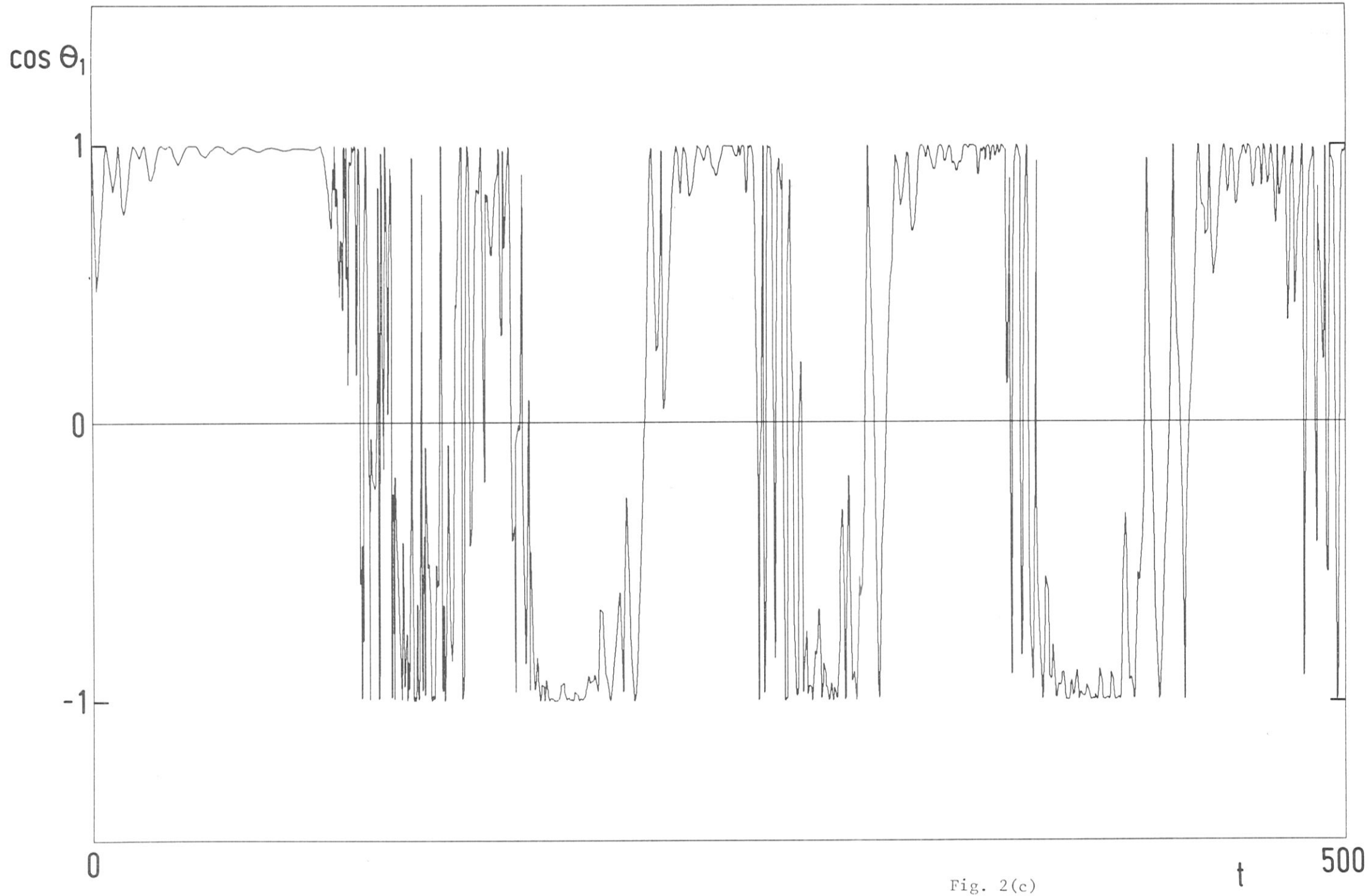

Fig. 2(c)

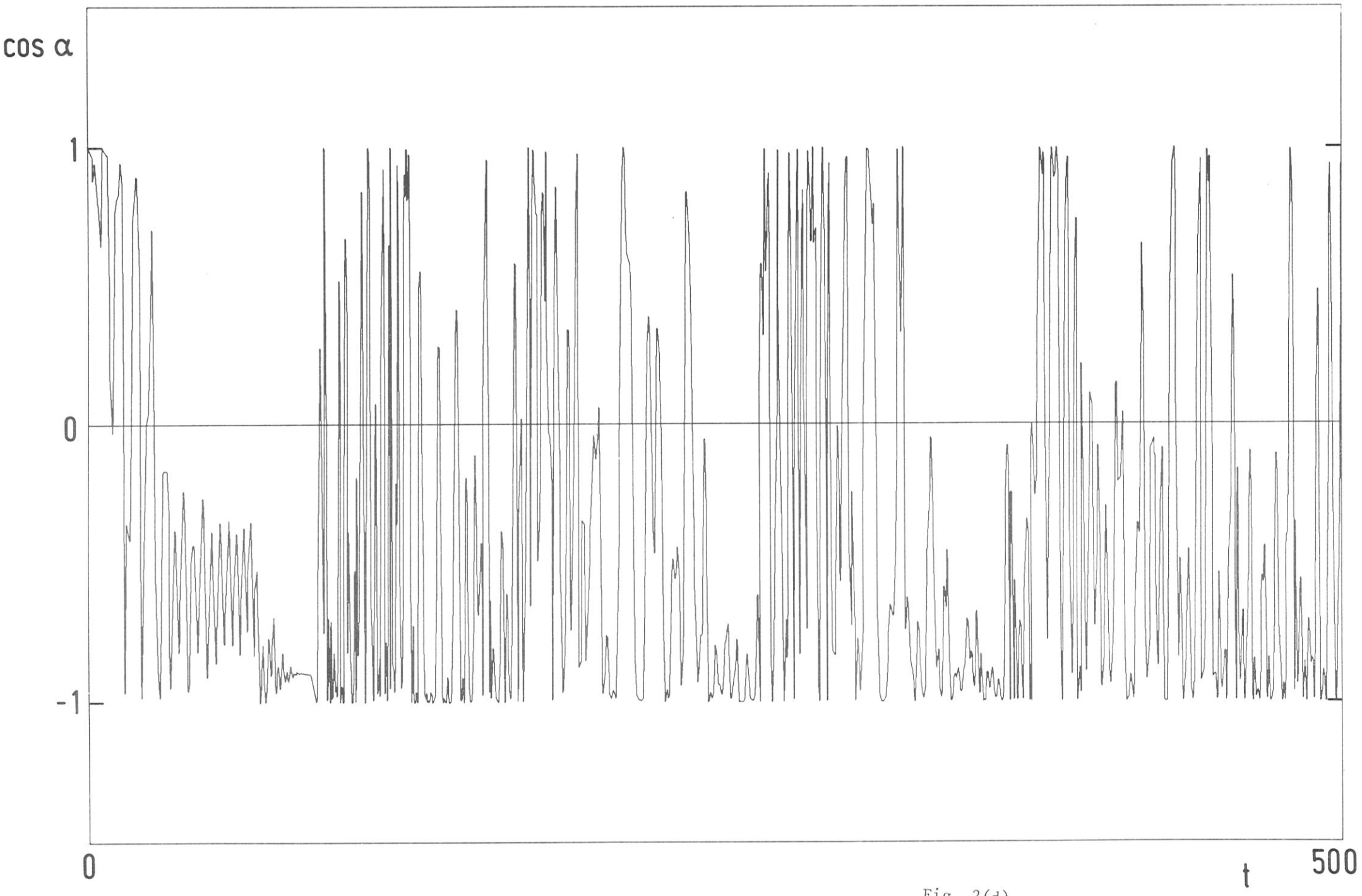

Fig. 2(d)

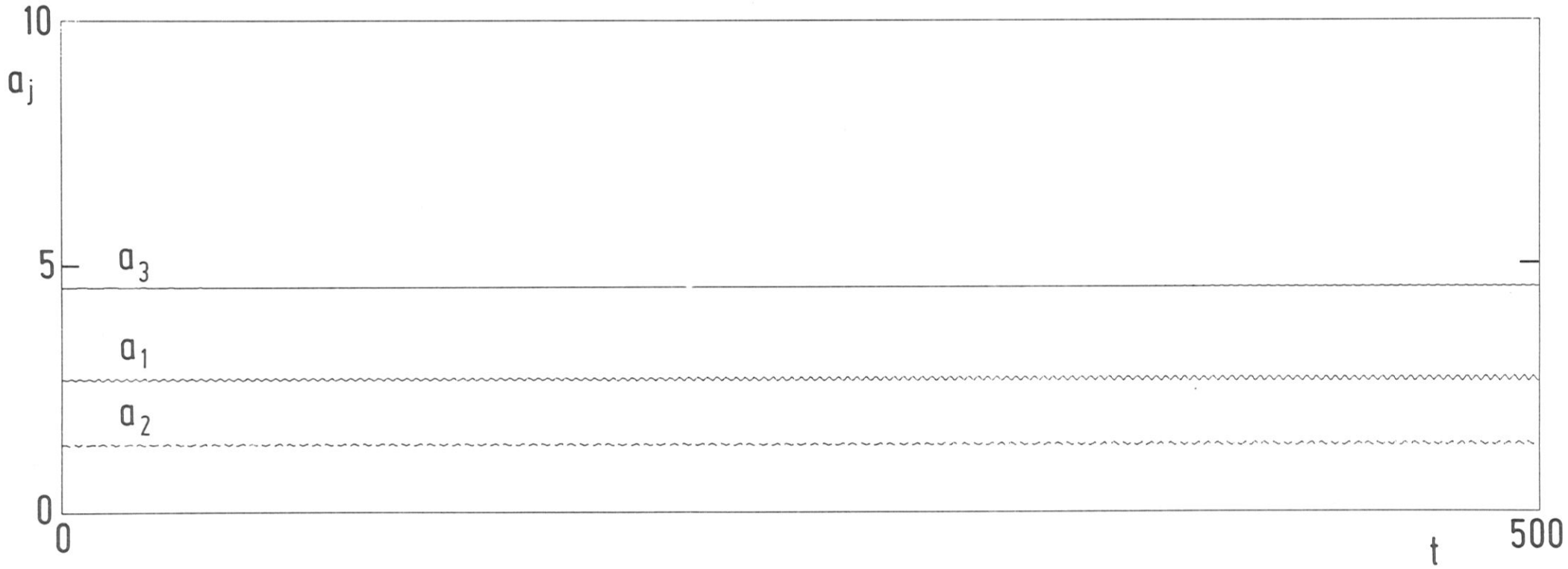

Fig. 3(a)

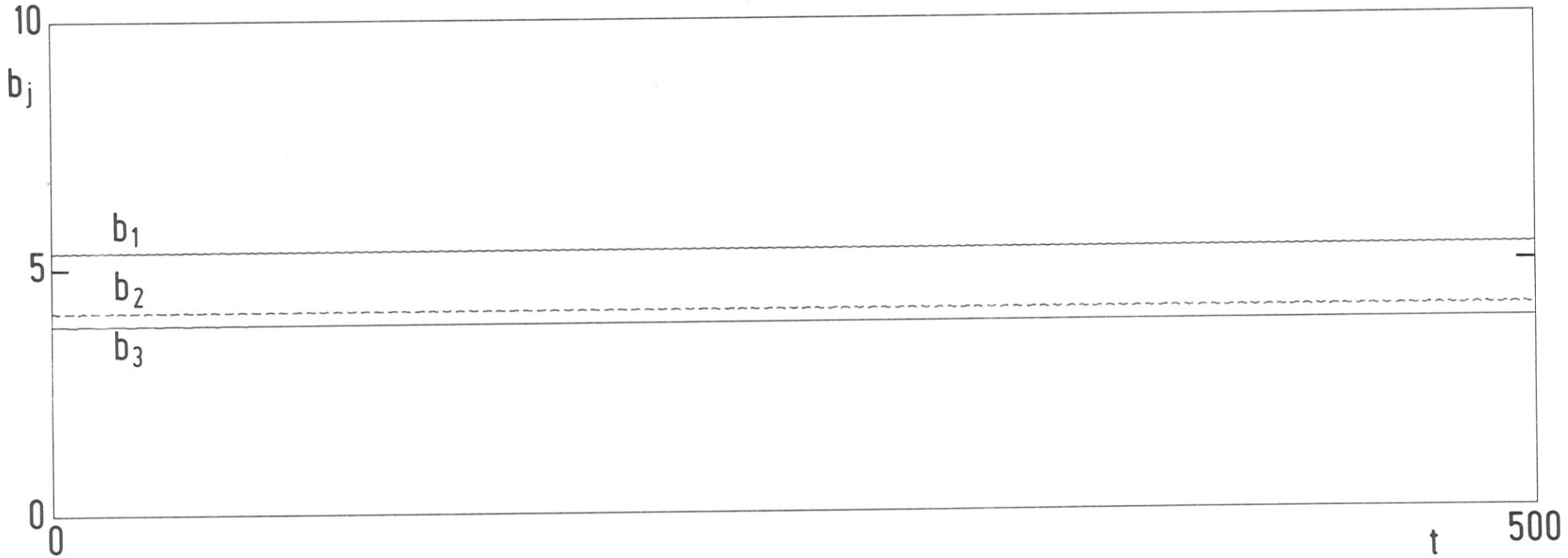

Fig. 3(b)

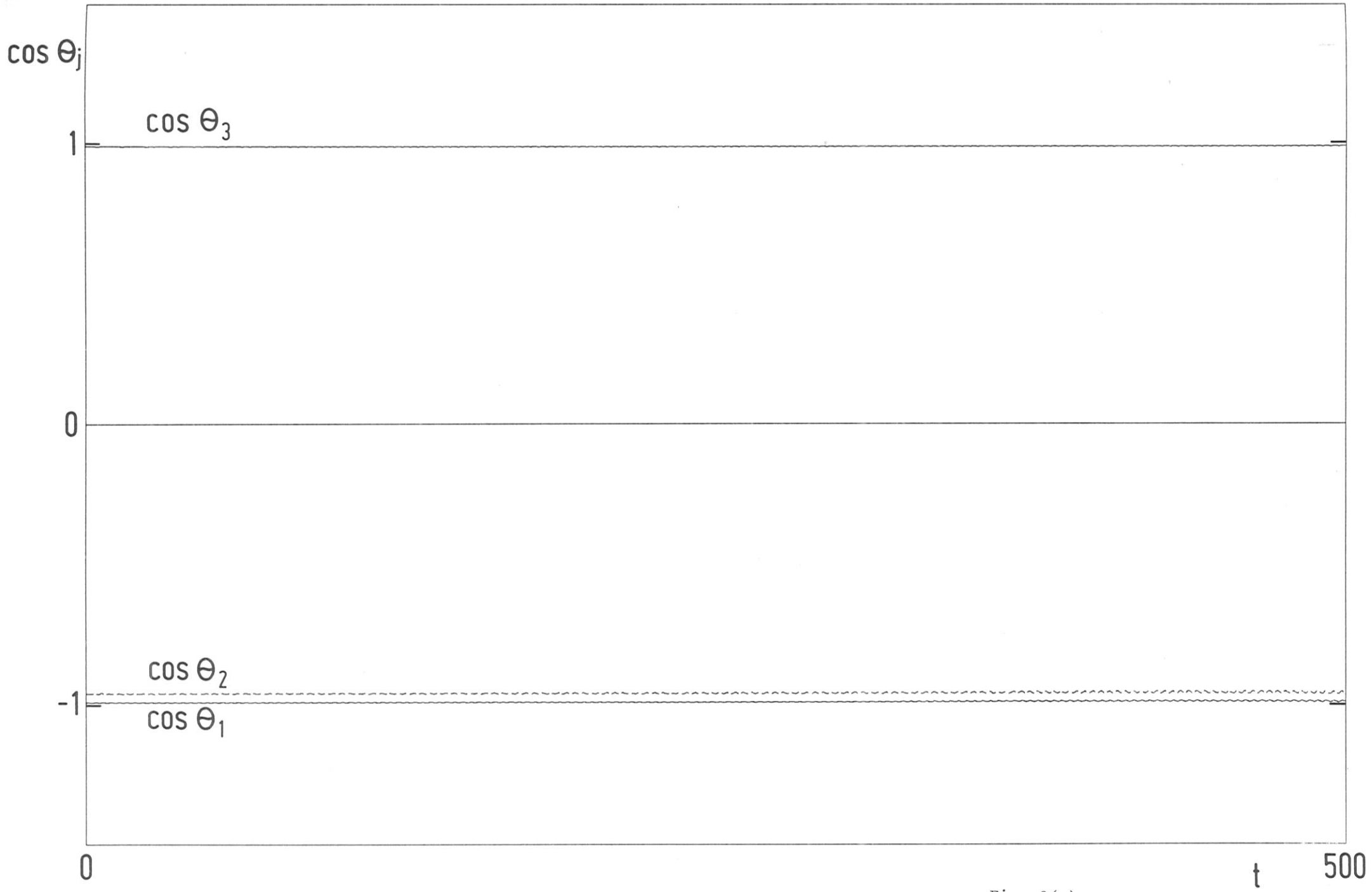

Fig. 3(c)

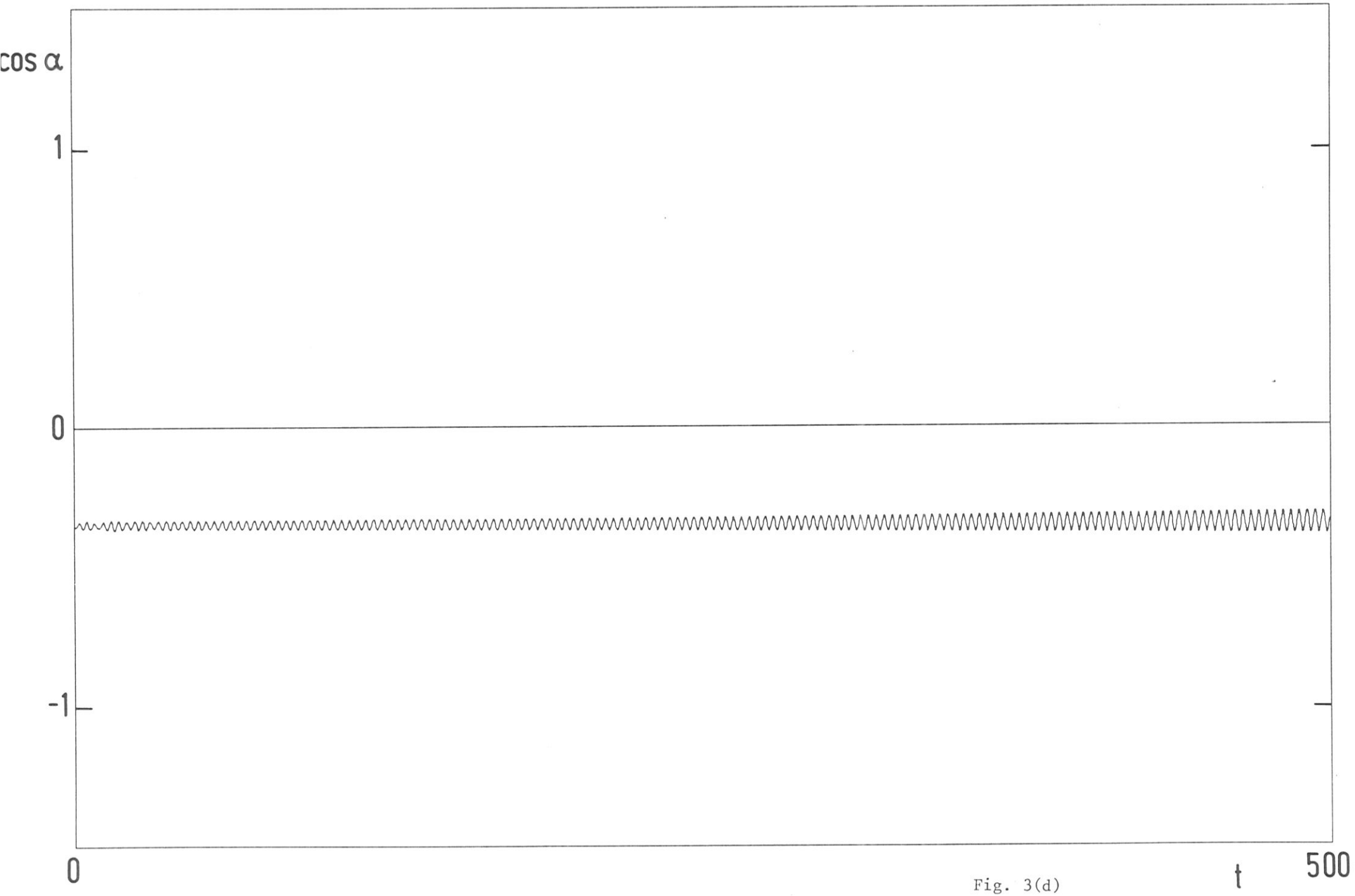

Fig. 3(d)

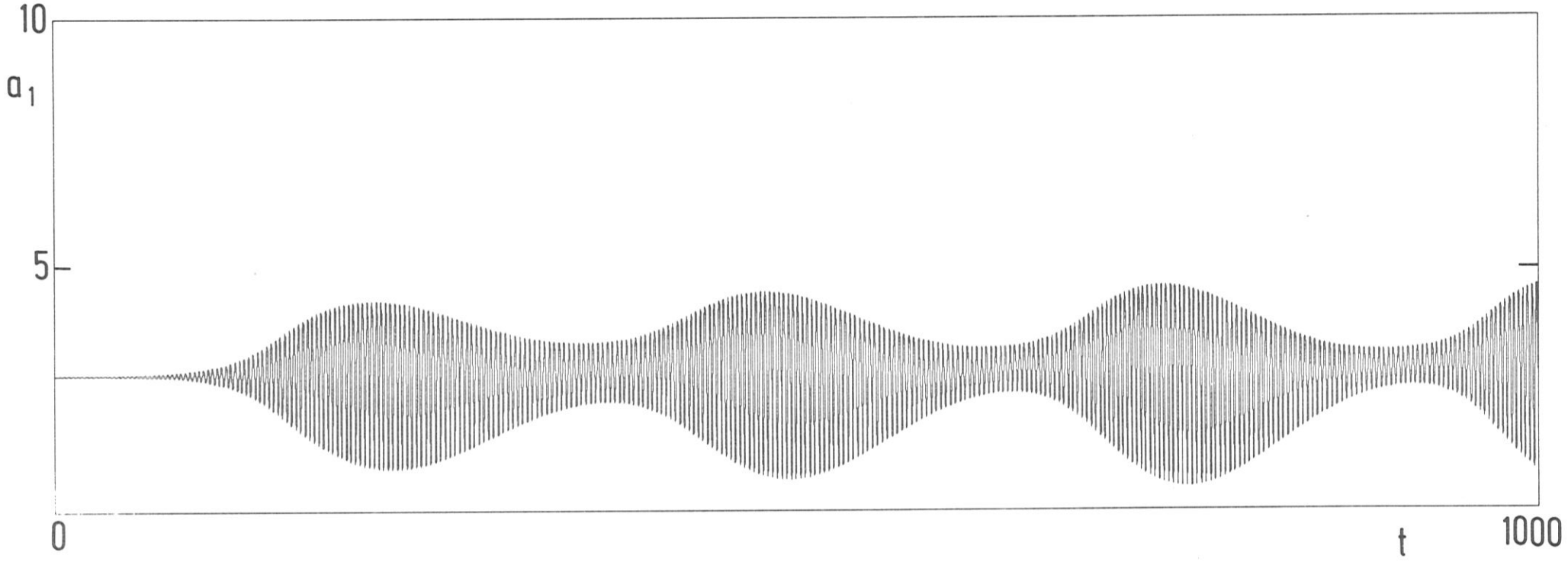

Fig. 4(a)

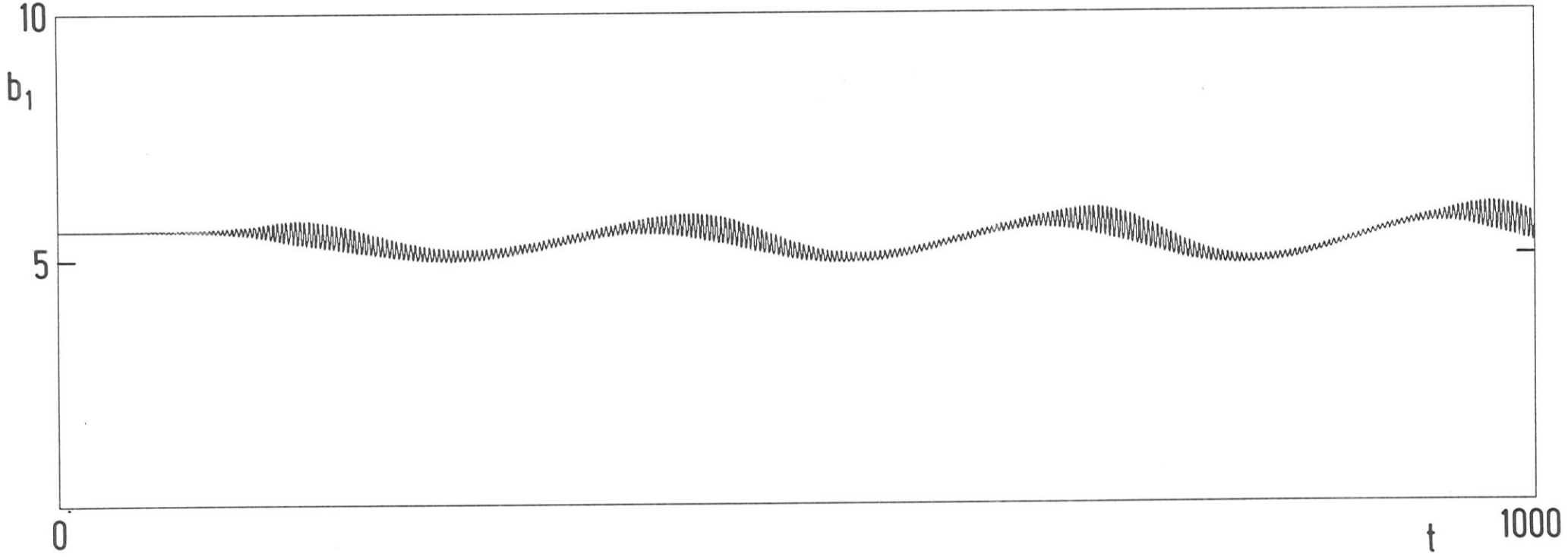

Fig. 4(b)

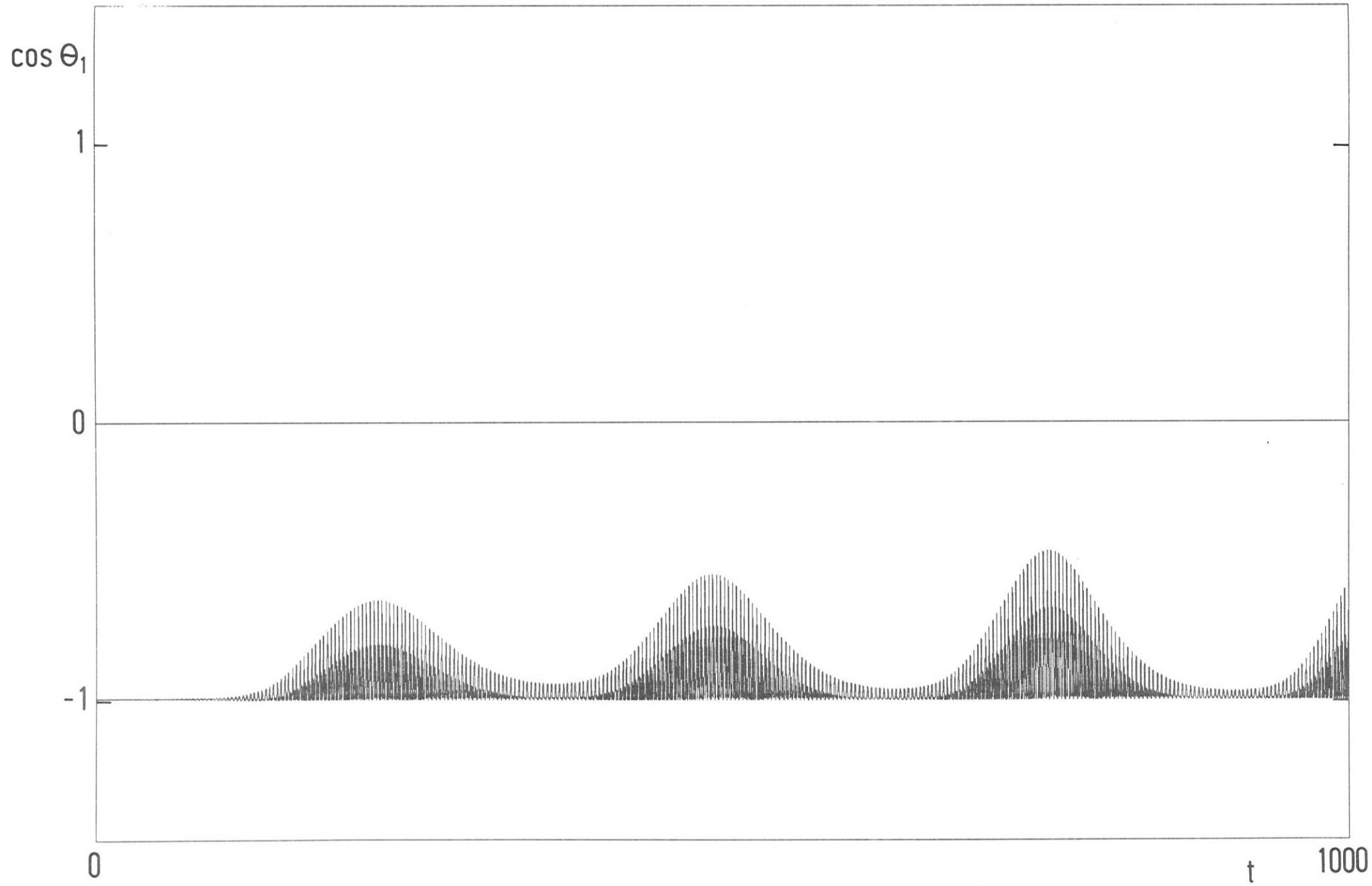

Fig. 4(c)

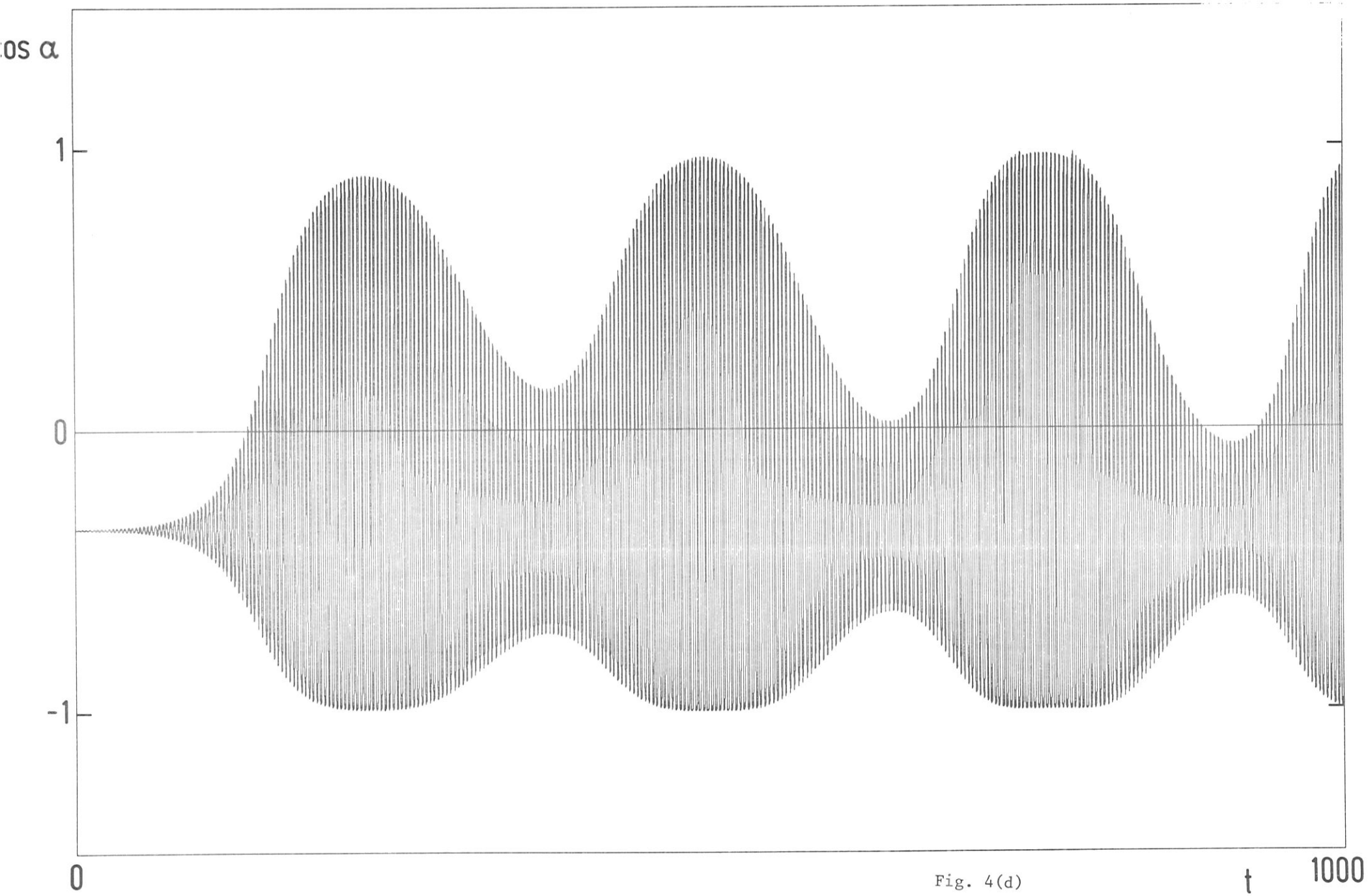

Fig. 4(d)

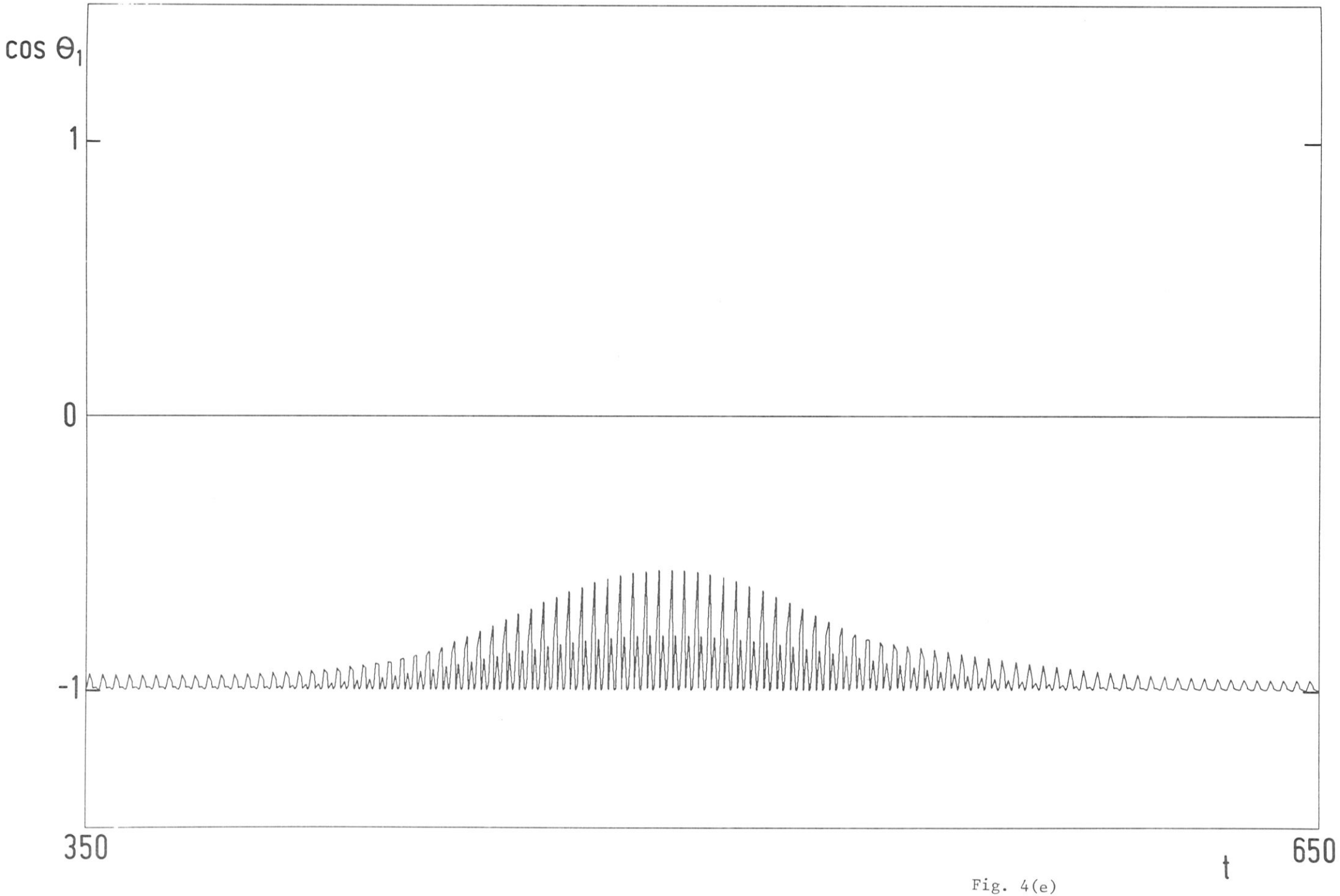

Fig. 4(e)

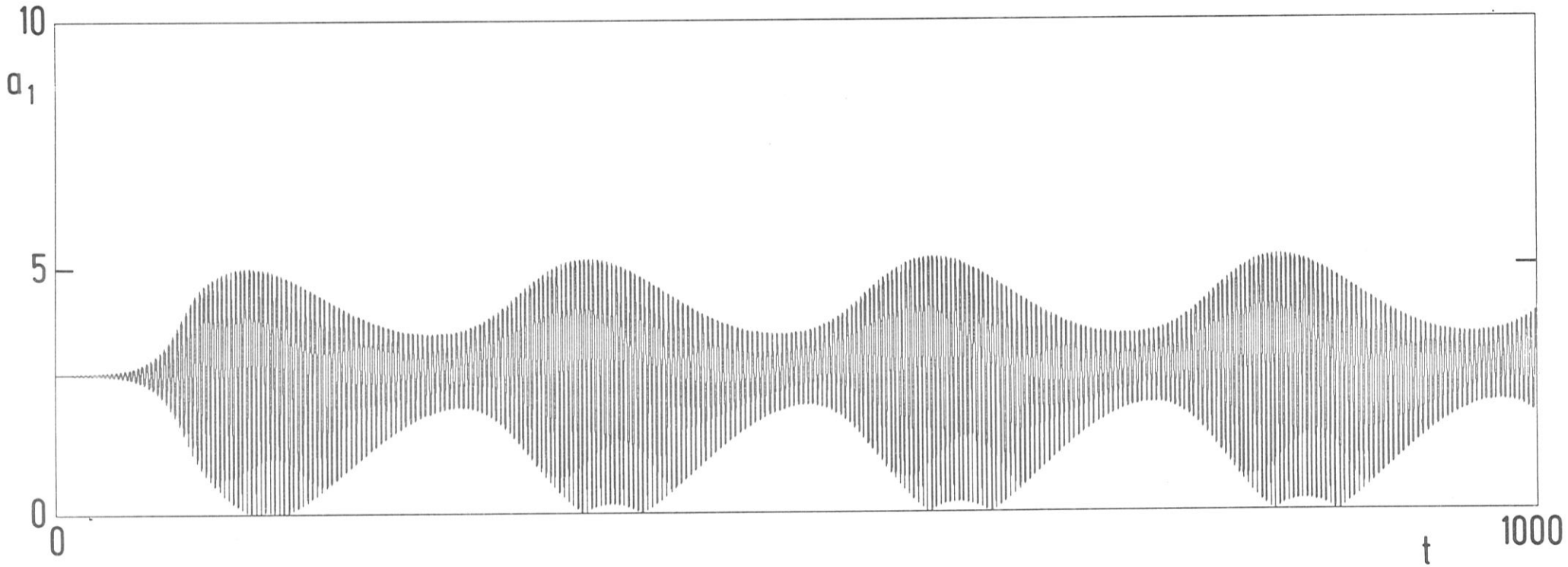

Fig. 5(a)

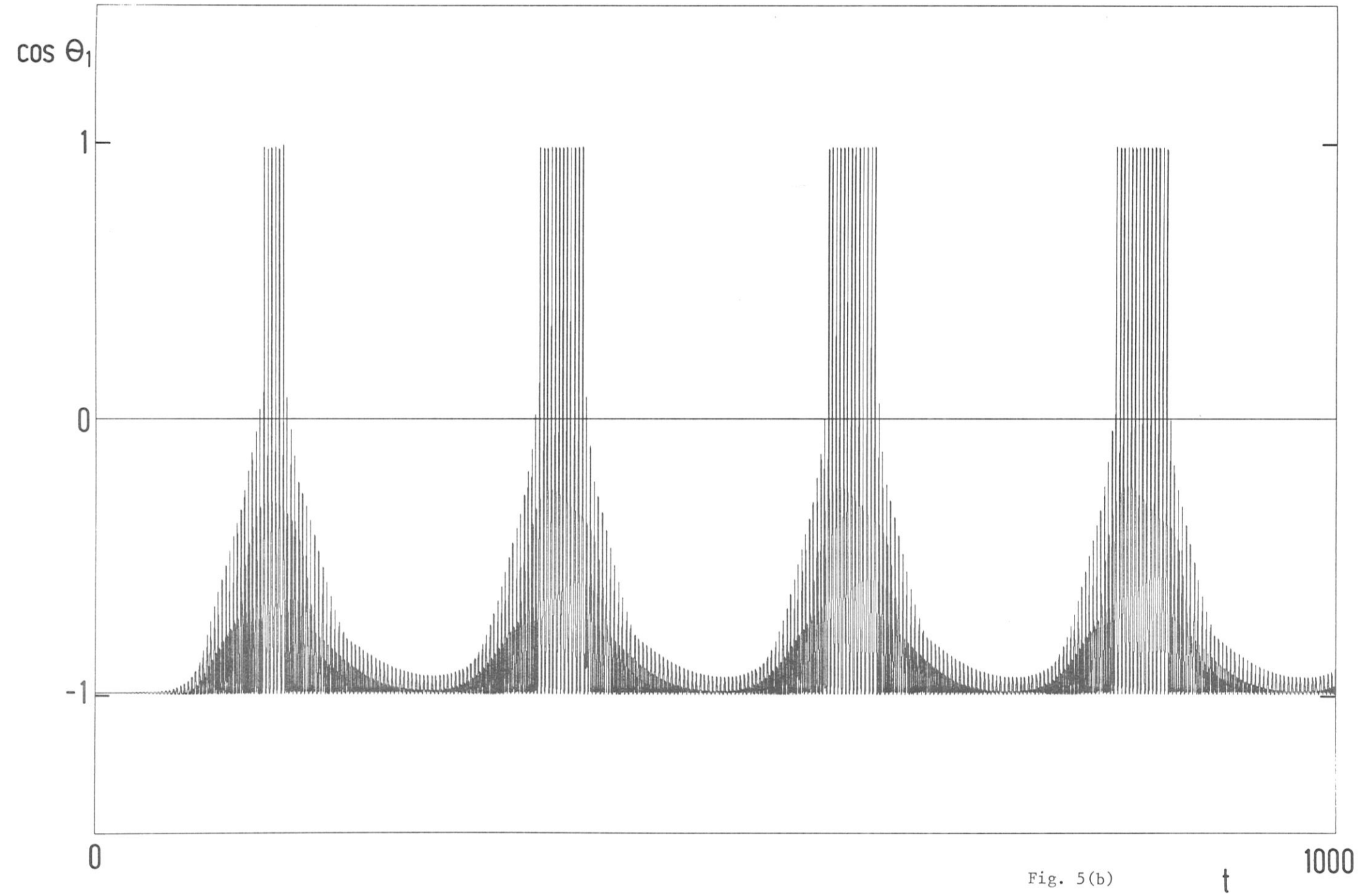

Fig. 5(b)

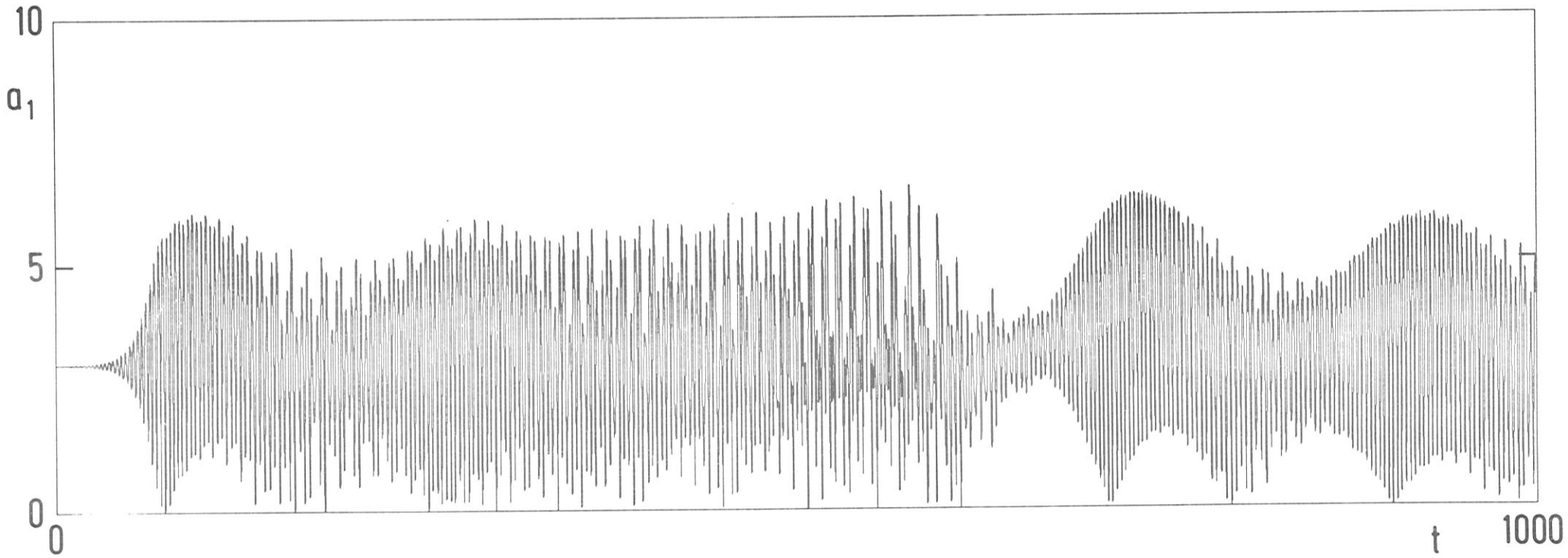

Fig. 6(a)

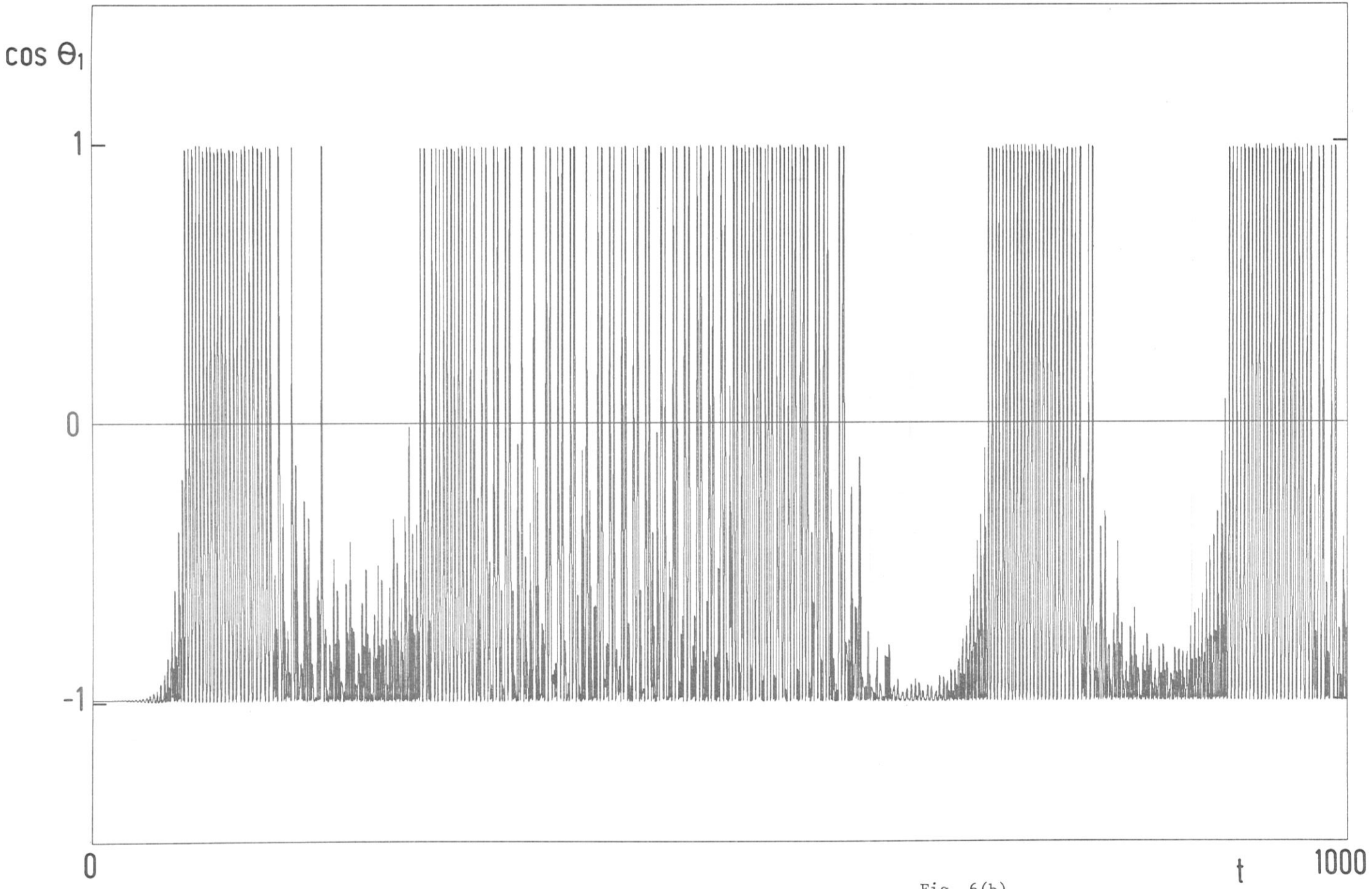

Fig. 6(b)

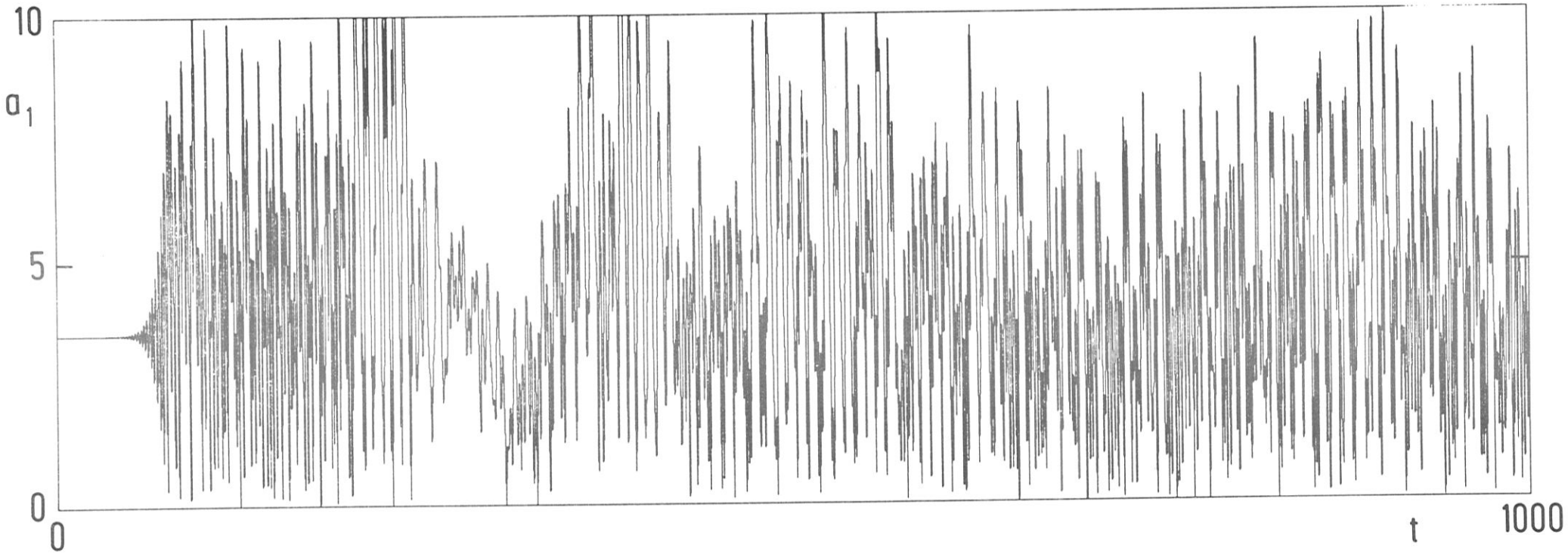

Fig. 7(a)

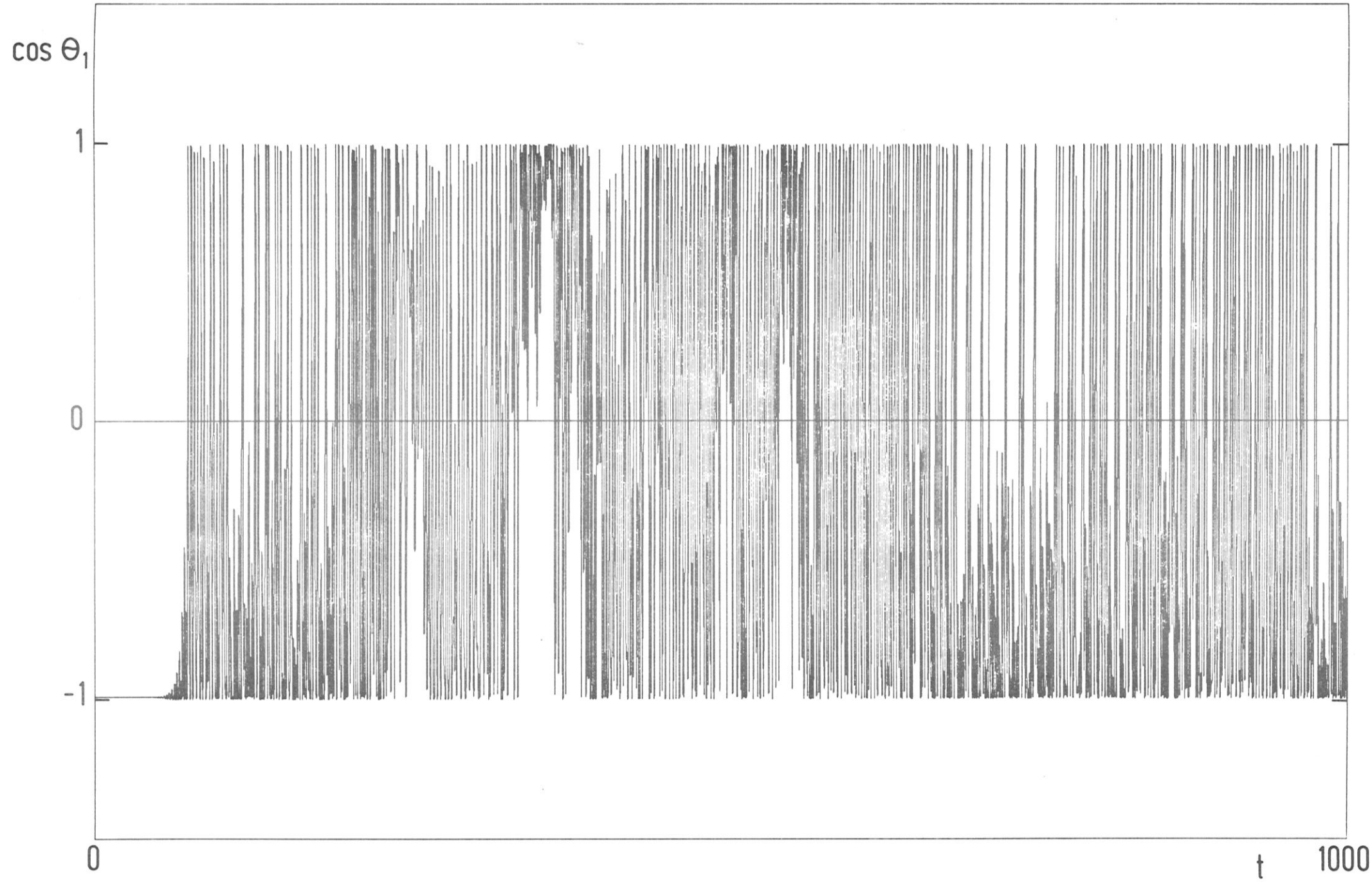

Fig. 7(b)

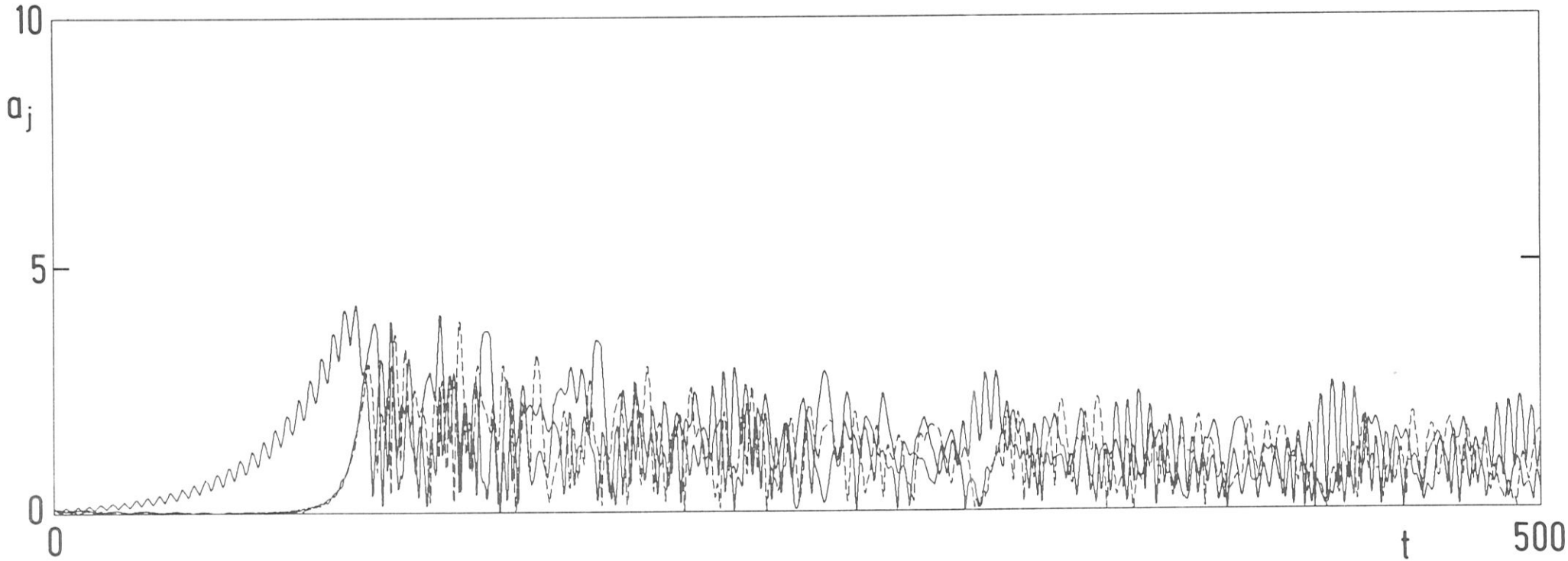

Fig. 8(a)

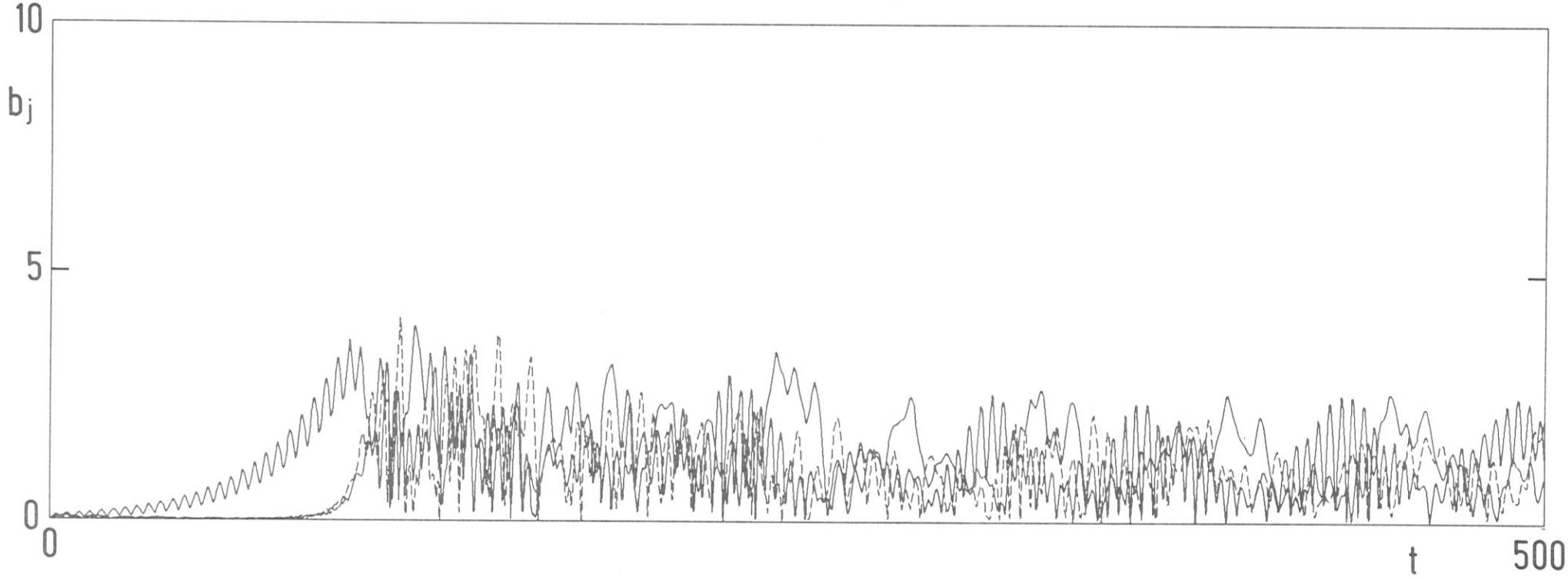

Fig. 8(b)

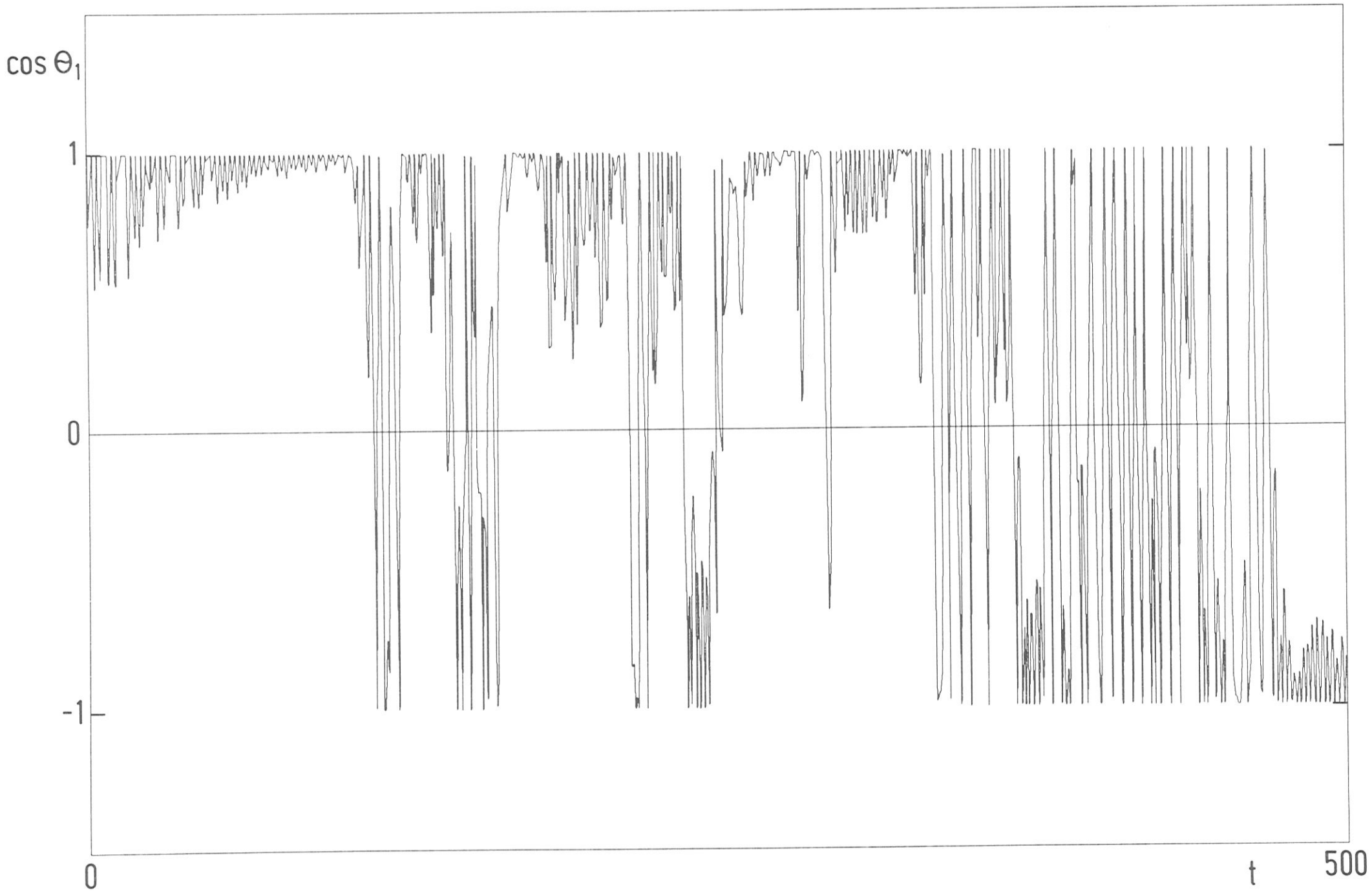

Fig. 8(c)

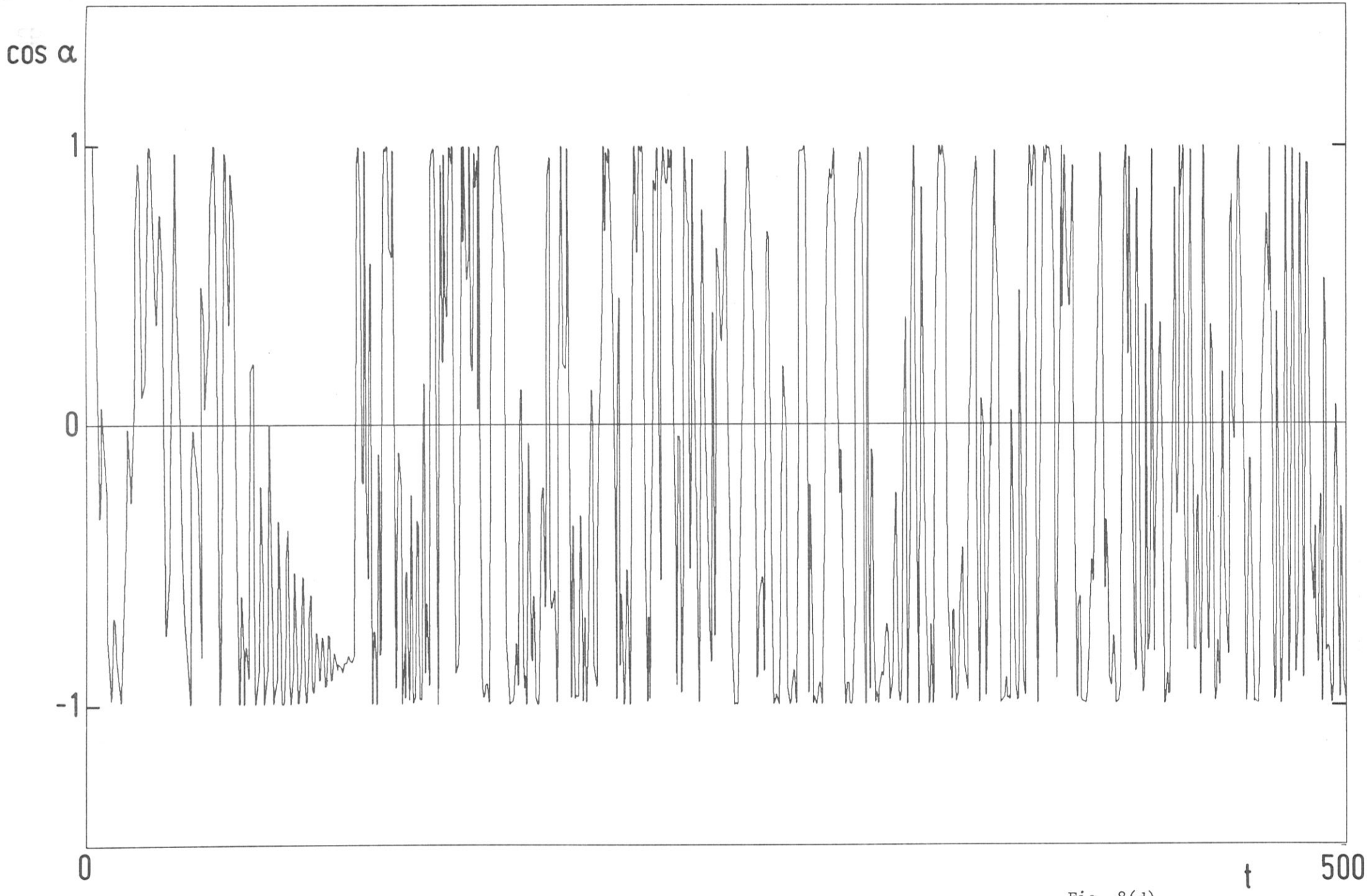

Fig. 8(d)

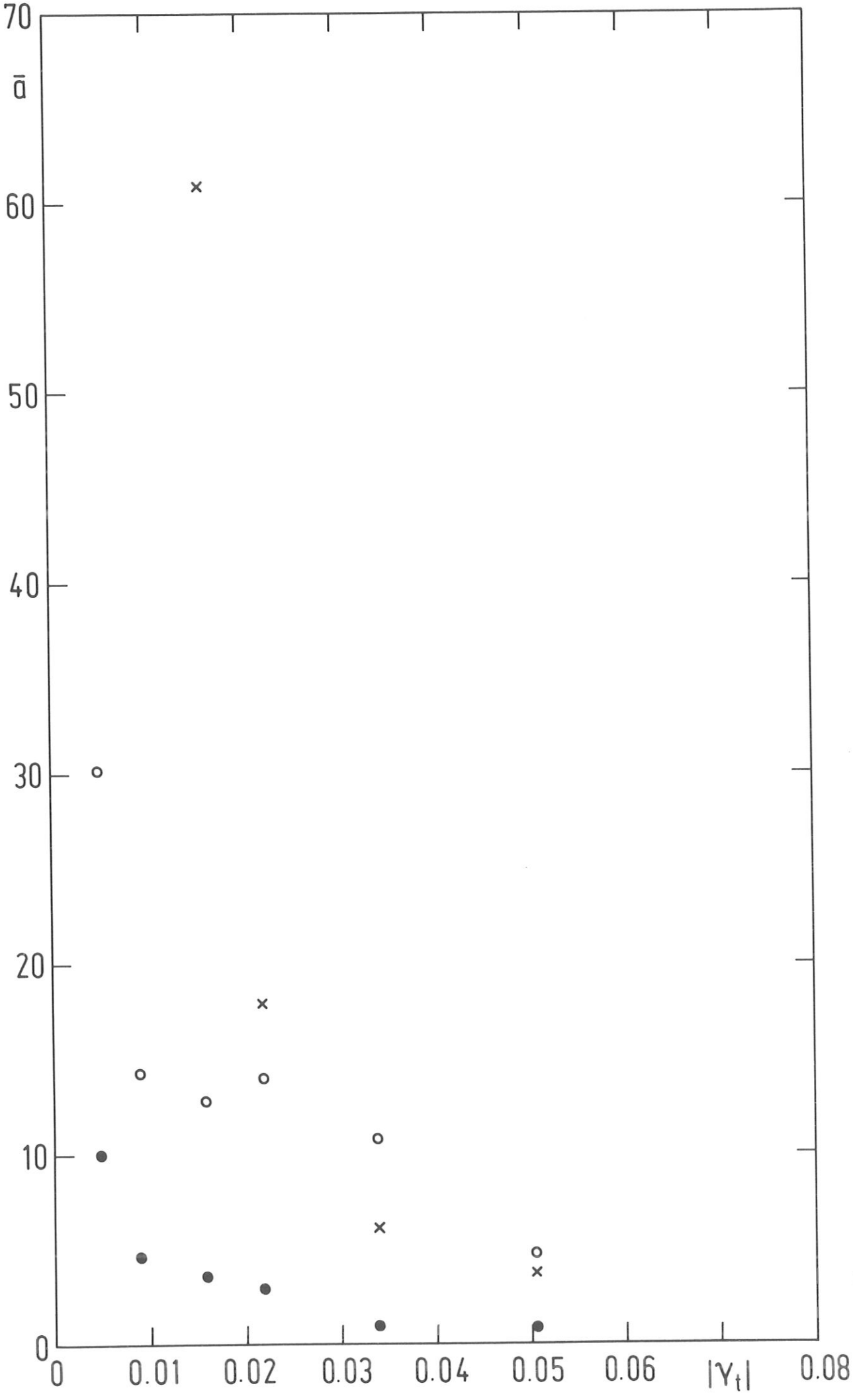

Fig. 9

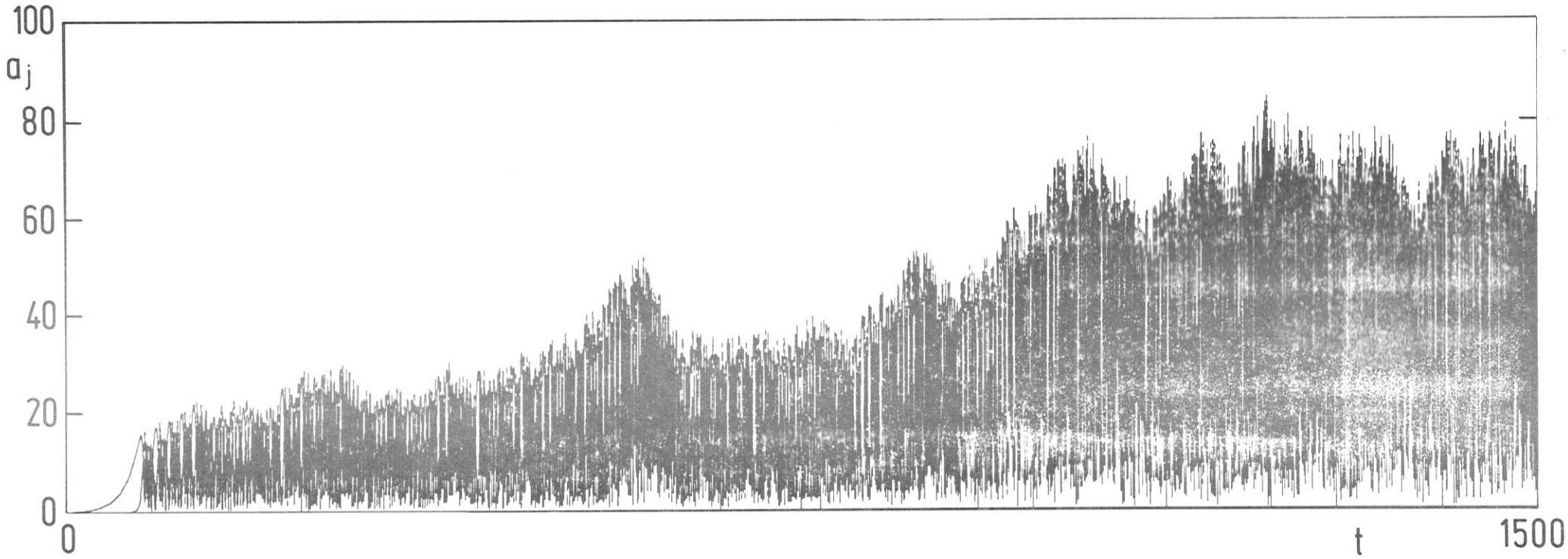

Fig. 10

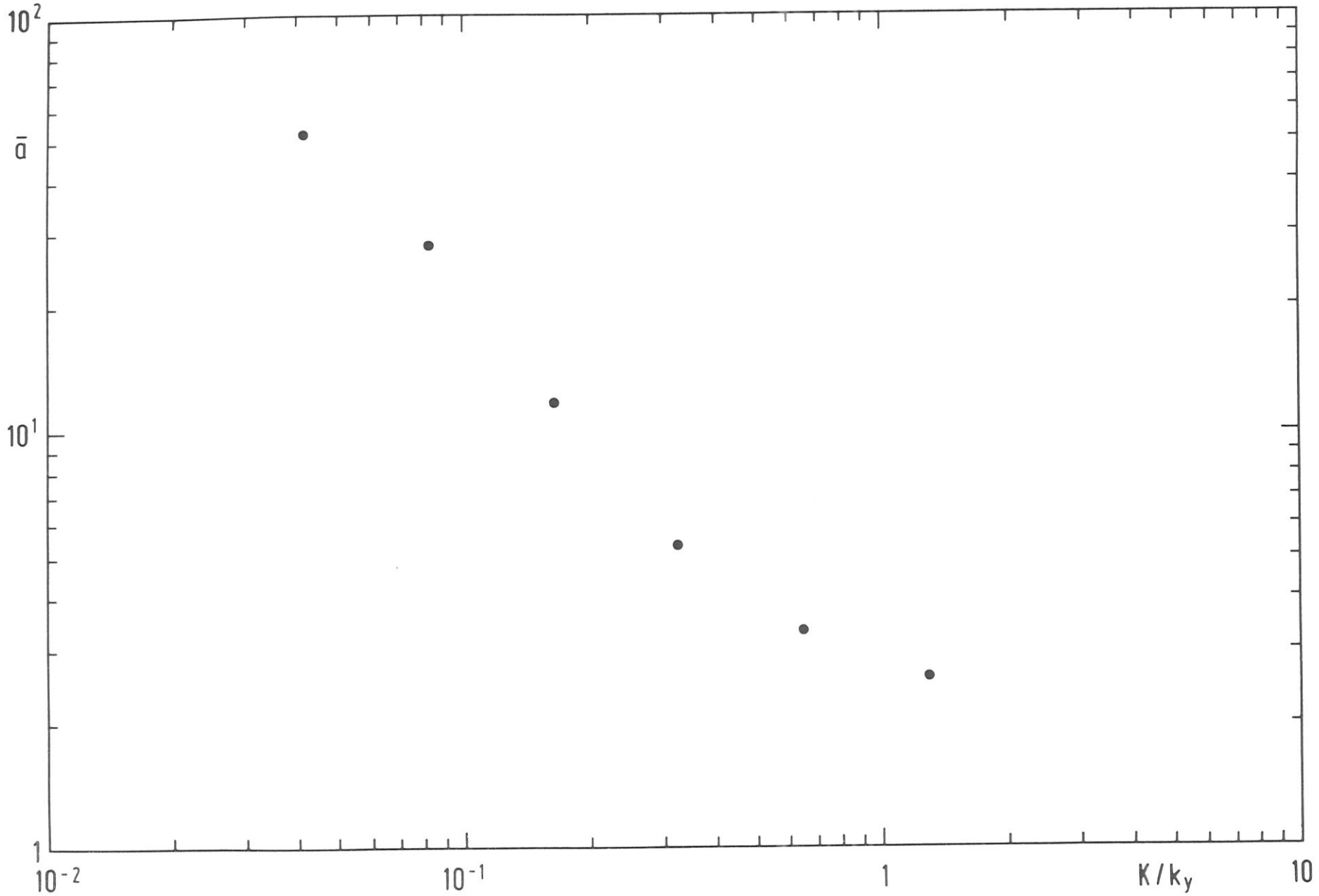

Fig. 11

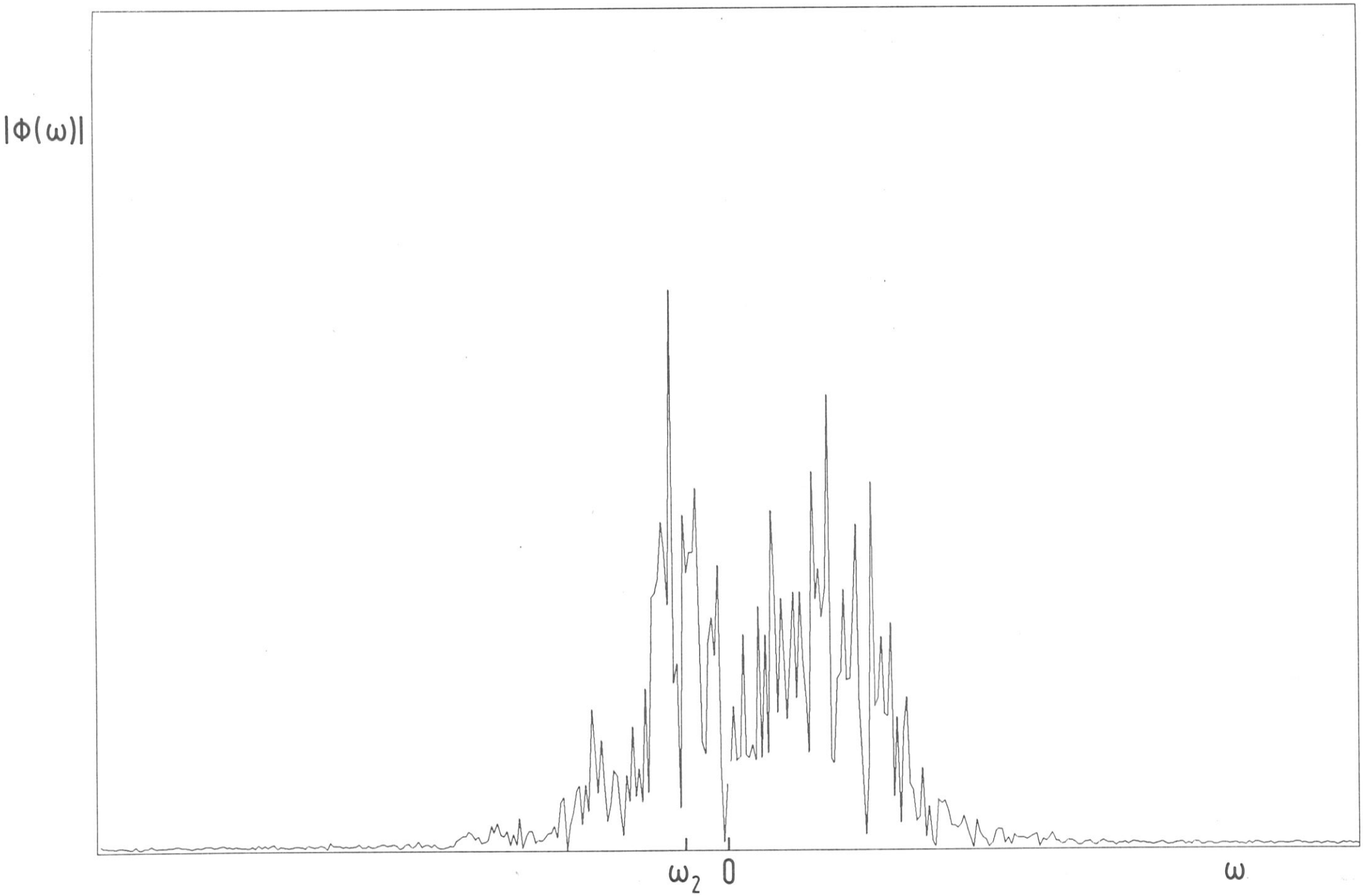

Fig. 12(a)

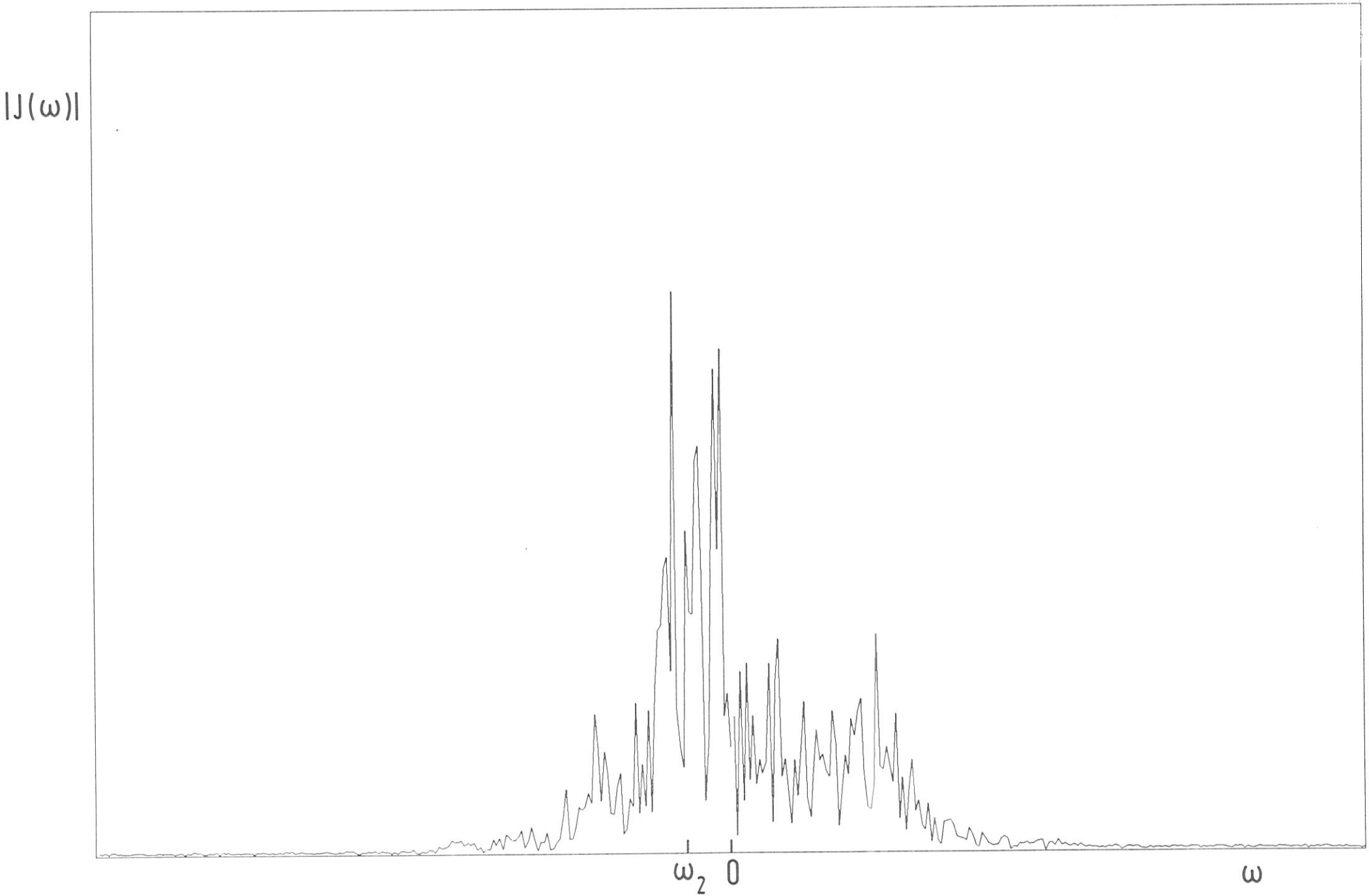

Fig.12(b)

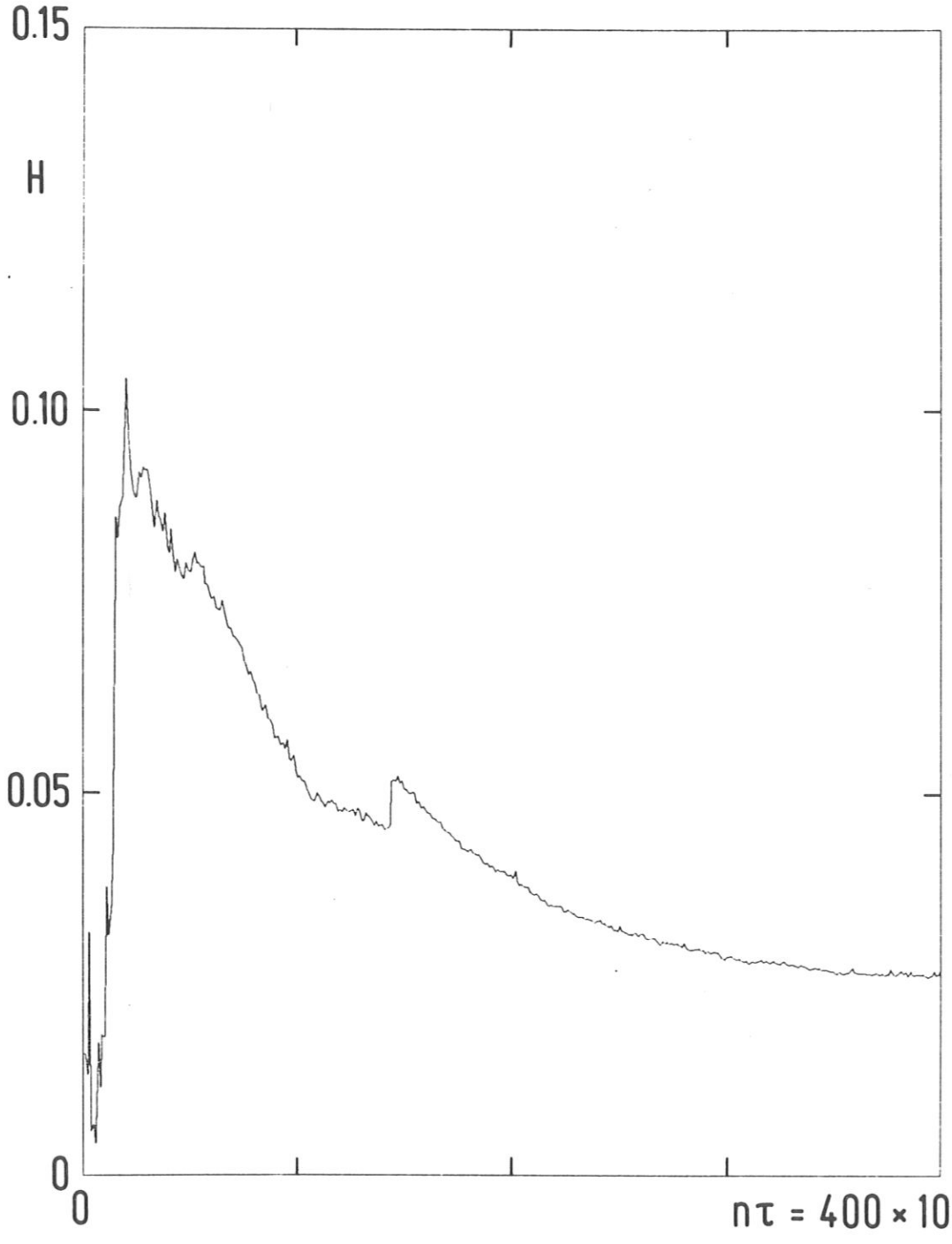

Fig. 13